Design for Local Member Shear at Brace and Diagonal-Member Connections: Full-Height and Chevron Gussets

RAFAEL SABELLI and BRANDT SAXEY

ABSTRACT

Large local member shear forces develop in beams in chevron-braced frames due to the delivery of brace forces to beam flanges, which are at a distance from the beam centerline (Fortney and Thornton, 2015, 2017; Hadad and Fortney, 2020). Using the "lower bound theorem" (Thornton, 1984), Sabelli and Arber (2017) developed design methods to address this local member shear by optimizing the internal stress distribution and thus maximizing the resistance utilized in design. This paper further develops those design methods for chevron beams and extends them to gusset connections at columns.

Keywords: gusset plates, braced frames, truss connections.

INTRODUCTION

The "chevron effect" is a term used to describe local beam forces in the gusset region of a chevron (also termed inverted-V) braced frame. These local forces are not captured by beam analysis methods that neglect connection dimensions. Fortney and Thornton (2015, 2017) and Hadad and Fortney (2020) have shown methods of analysis for these forces. This study adds design solutions for addressing high member shear in the connection region, including reinforcement and proportioning for (chevron) gussets within the beam span and for full-height gussets at beam-column-brace connections.

V-braced frames (and their variants) are commonly used in steel structures and are commonly termed "chevron-braced frames." Figure 1 shows three chevron configurations: the inverted-V-braced frame (a), in which two braces connect to the bottom of the beam at its midpoint; the V-braced frame (b), in which two braces connect to the top of the beam at its midpoint; and the two-story, X-braced frame (c), in which four braces connect to the beam at its midpoint, two from above and two from below.

The beams and columns of these frames are typically designed using centerline models, and equilibrium is addressed in the design at the "workpoint" (the intersection of member centerlines). In typical design, a substantial gusset plate is provided at brace connections, and force transfer is accomplished over the length of that plate. Figure 2 shows a frame with such gusset plates. Similar connections

Rafael Sabelli, Director of Seismic Design, Walter P Moore, San Francisco, Calif. Email: rsabelli@walterpmoore.com (corresponding)

Brandt Saxey, Technical Director, CoreBrace, West Jordan, Utah. Email: brandt.saxey@corebrace.com

Paper No. 2020-01

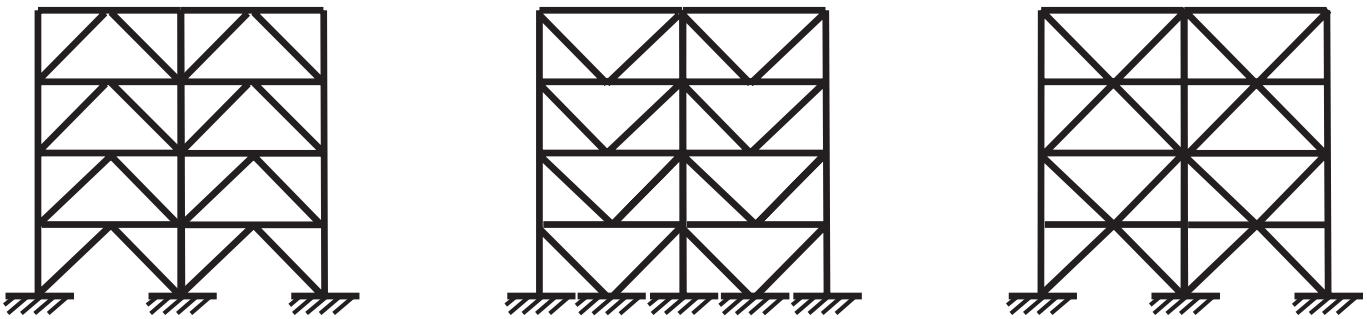

(a) Inverted-V-braced frame *(b) V-braced frame* *(c) Two-story, X-braced frame*

Fig. 1. Chevron-braced frame configurations.

are used in truss construction with web-vertical wide-flange chords (Figure 3).

Work by Fortney and Thornton (2015, 2017) and Hadad and Fortney (2020) highlights the importance of analysis of chevron braced-frame connections. In particular, Fortney and Thornton derive expressions for the local beam shear and moment that result from the distribution of brace forces over the gusset-plate length. These beam forces (in particular, the shear) can result in the need to supplement the beam web with a doubler plate. An example of such a condition is shown in the second edition AISC *Seismic Design Manual* (AISC, 2012). In the third edition *Seismic Design Manual* (AISC, 2018), the example connection utilizes some of the relationships developed by Sabelli and Arber (2017) to eliminate the need for reinforcement.

This study builds on the work of Sabelli and Arber, applying the same concepts developed by Fortney and Thornton, with the aim of providing methods for the design of connections that do not require reinforcement. The methods presented in this paper rely heavily on the "lower bound theorem" as presented by Thornton (1984) for similar connections, demonstrating adequate strength through investigation of an advantageous internal stress distribution in a ductile connection and examining forces at gusset edges and at critical sections.

This study also extends and generalizes the equations developed for chevron connections for use in other conditions, such as columns with full-height gussets (also called "mega-gussets") in which the gusset extends through the beam depth and the beam connects to the gusset rather than to the column (see Figure 4). In addition to transferring brace forces, full-height gusset connections transfer beam forces to the column. Such connections may be accomplished with welded beam flanges (as shown in Figure 4), which provide flexural continuity (and thus additional flexural forces to be transferred by the gusset to the column), or with a connection similar to a single-plate connection (also known as a "shear tab"), which minimizes these flexural forces. Adaptation of these methods to beam-column-brace connections with traditional gussets (Figure 5) is beyond the scope of this paper.

The first part of the paper derives the design equations employing statics and two models of stress distribution along the gusset-flange interface: the Uniform Stress Method, based on Fortney and Thornton (2015), and the Concentrated Stress Method, based on Sabelli and Arber (2017). The former model is simpler, but if that model indicates that reinforcement is required, significant economy can be realized by using the latter. The second portion of the paper is a brief design example that addresses both methods for the design of a chevron connection.

This study addresses both member shear and member moment caused by the local connection forces as these differ from the shears and moments from a simple, centerline model of members. In the authors' experience, the local member shear often controls the connection design (such as by necessitating a minimum gusset length), but the additional member moment caused by the local connection forces does not.

The design equations derived here are based on the static equilibrium of the gusset plate based on the brace axial forces (and beam reactions for the column connection). As such, they are equally applicable to frames designed as part of a ductile seismic system (in which brace forces typically correspond to the brace capacity), and those designed for wind or other cases that do not involve capacity design. Additional considerations for seismic design, such as determination of the appropriate brace force level for which beam yielding should be precluded, are beyond the scope of this paper.

Fig. 2. Typical braced frames with gussets.

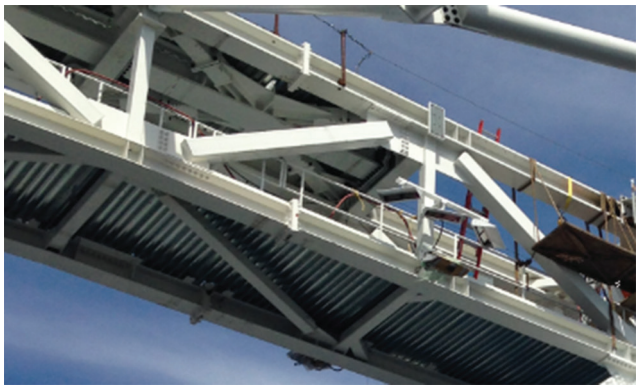

Fig. 3. Truss with gussets.

Fig. 4. Full-height gusset brace connection at column.

Fig. 5. Traditional gusset at column.

SYMBOLS, NOMENCLATURE, AND CONVENTIONS

This study employs the following symbols and terms:

D_{clip} Diagonal dimension of reduced critical-diagonal-section length due to $Y_{clip,}$ in. (mm)

D_{crit} Length of critical diagonal section of gusset, in. (mm)

$F_{i,j}$ Brace axial force for brace "j" connecting to gusset "i," kips (N) (sign conventions are per the figures)

F_N Gusset concentrated force at member flange, transverse to member axis, kips (N) (compression is positive)

F_V Gusset shear component parallel to member axis at interface with flange, kips (N)

F_{Xcrit} Force parallel to the member axis acting on critical diagonal section of gusset, kips (N)

F_{Ycrit} Force transverse to member axis acting on critical diagonal section of gusset, kips (N)

F_y Specified minimum yield stress, ksi (MPa)

L_{beam} Beam length (column centerline to centerline), in. (mm)

L_g Gusset length, in. (mm)

L_w Length of weld, in. (mm)

M_{Bm} Beam moment transferred to gusset at column connection, kip-in. (N-mm)

M_{Ch} Chevron moment at face of member due to force F_V (equal and opposite to the distributed moment M_{FV} for concentric workpoints), kip-in. (N-mm)

M_{crit} Moment acting on critical diagonal section of gusset, kip-in. (N-mm)

M_f Moment at gusset-to-flange-interface due to brace forces, kip-in. (N-mm)

M_{FV} Moment in the connection due to force F_V, distributed along gusset length and eccentric to workpoint (equal and opposite to the chevron moment, M_{Ch}, for concentric workpoints), kip-in. (N-mm)

M_g Moment on a gusset section transverse to the member axis, kip-in. (N-mm)

M_M Member moment at workpoint due to loading other than from braces, kip-in. (N-mm).

M_n Nominal member or element flexural strength, kips (N)

M_{max} Maximum member moment (within connection region) due to brace forces, kip-in. (N-mm)

M_{Tot} Total moment acting on beam due to M_{f1} and M_{f2}, kip-in. (N-mm)

N_{Bm} Beam axial force transferred to gusset at column connection, kips (N)

N_g Normal force on a gusset section transverse to the member axis, kips (N)

P_n Nominal member or element axial strength, kips (N)

R_u Required strength, kips (N)

R_z Normal force from moment transfer for Concentrated Stress Method, kips (N)

V_{Bm} Beam connection shear transferred to gusset at column connection, kips (N)

V_{Ch} Chevron shear, equal to the sum of member shear and gusset shear transverse to member axis, kips (N)

V_{ef} Effective member shear strength (deducting demands other than brace connection forces), kips (N)

V_{efTot} Effective member shear strength considering the effects of unbalanced forces from gussets on both sides of the member, kips (N)

V_g Shear on a gusset section transverse to the member axis, kips (N)

V_M Member shear due to loading other than from braces, kips (N)

V_{ma} Member shear (outside connection region), kips (N)

V_{mc} Member shear (within connection region), kips (N)

V_n Nominal member or element shear strength, kips (N)

W Width of brace-to-gusset connection used to locate critical diagonal section, in. (mm)

X_{crit} Dimension parallel to the member axis used to locate critical diagonal section, in. (mm)

Y_{clip} Dimension transverse to member axis of gusset corner clip, in. (mm)

d_m Member depth, in. (mm)

d_g Gusset dimension transverse to member axis, in. (mm)

e_{crit} Location of force F_{Ycrit} with respect to intersection of critical diagonal section and gusset edge, in. (mm)

e_g Eccentricity parallel to member axis of gusset midpoint from workpoint (e.g., beam centerline at column connection), in. (mm)

e_m Transverse eccentricity from member flange to workpoint, typically equal to half the member depth, in. (mm)

e_z Length of moment arm between centroids of z regions, in. (mm)

k Distance from outer face of flange to web toe of fillet, in. (mm)

r_u Required strength per unit length, kips/in. (N/mm)

t_g Gusset thickness, in. (mm)

t_w Member web thickness, in. (mm)

w Weld size, in. (mm)

x Distance from gusset midpoint along member axis, in. (mm)

z Length of concentrated stress region at ends of gusset, in. (mm)

γ Brace angle from member longitudinal axis, deg

ϕ_b Resistance factor for bending (0.9)

ϕ_c Resistance factor for compression (0.9)

ϕ_n Resistance factor for nonductile limit states such as web crippling and weld rupture (0.75)

ϕ_t Resistance factor for tension (0.9)

ϕ_w Resistance factor for web local yielding (1.0)

ϕ_v Resistance factor for shear (1.0)

Subscripts are employed in some equations to distinguish actions and dimensions related to one gusset or one brace from another. Gussets are designated "1" and "2," and dimensions and forces associated with each gusset are given the corresponding subscript. The subscript "*Tot*" refers to total forces, combining those from gusset "1" and gusset "2."

Brace axial forces have two subscripts. The first pertains to which gusset the brace connects to ("1" or "2"). The second pertains to which of the two braces is indicated. Sign conventions match the figures such that positive brace axial forces $F_{1,2}$ and $F_{2,1}$ correspond to compression and positive brace axial force $F_{1,1}$ and $F_{2,2}$ correspond to tension. Forces and angles pertaining to each brace carry the same designation subscript.

The design equations are presented in a general form such that they can be used for both column and beam gussets. To permit this, certain general terms are used, such as "member" in lieu of "beam" or "column." This approach carries through to the symbols.

Brace-force components acting on the gusset–member interface are described as (gusset) "shear" or "normal" forces. Gusset shear forces, F_V, are parallel to the member axis (horizontal for the chevron beam and vertical for the column); normal forces on the connection, F_N, are perpendicular to the member axis (vertical for the chevron beam and horizontal for the column).

The term "workpoint" refers to the intersection of brace centerlines with each other or with the column centerline. This workpoint is typically also at the beam centerline.

Figure 6 shows dimensions noted on beam and gusset-plate diagrams. Braces may occur above the beam, below the beam, or both. The diagram shows a symmetrical condition, but the connection calculations apply for asymmetrical cases. (Beam shear and moment require adjustment for asymmetrical applications.) Figure 7 shows dimensions noted on column and gusset-plate diagrams. Braces may occur in various combinations, and the column may continue up past the connection or may terminate as shown in the upper diagram. The diagram shows a full-height gusset: a gusset plate that comes between the beam and the column.

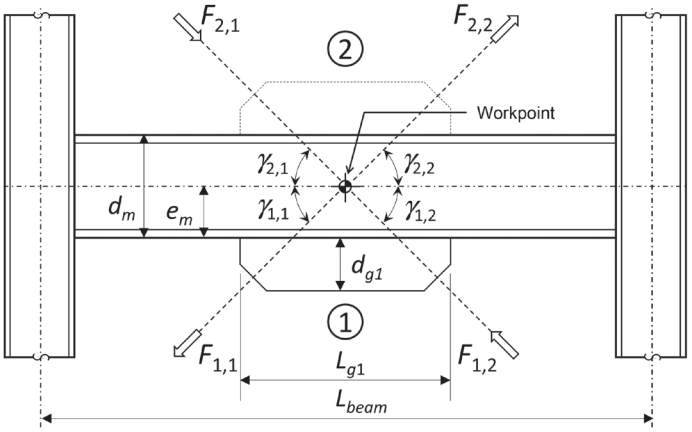

Fig. 6. Chevron gusset geometry.

STATICS

Although the methods developed in this paper are intended to facilitate the design of connections of multiple members (such as is shown in Figure 7), in essence the methods simply provide designers with the means of designing an attachment to a wide-flange member (such as is shown in Figure 8) for a set of known, in-plane forces, converting these to a normal force transverse to the member axis, F_N, a shear force parallel to the member axis, F_V, and a moment in the plane of the web, M_f. The design of this connection includes evaluation of local limit states within the member, including web local yielding, web crippling, and local shear. This local shear (in the gray zone in the center diagram in Figure 8) is essentially panel-zone shear, and determination of the effective depth of the force couple is central to the design methods presented. The right-hand diagram in Figure 8 illustrates that while the member flange and bracket rotate in unison, the panel-zone section of the member web can undergo large shear strains while the bracket remains elastic, and thus the member can yield in shear even if there is a substantial bracket present. The shear strength of the member is not increased by the addition of the bracket shear strength; a thicker or wider bracket would not preclude panel-zone shear yielding. Instead, the shear demand on the member panel zone can be reduced by using a bracket that extends further along the flange, thus increasing the height of the panel zone.

The same reconstitution of forces is applicable to braced-frame and truss connections, assuming the forces in the connecting members are known. The analysis and design of braces and truss diagonals is typically based on their idealization as pin-pin members. In some cases, this idealization could be modified to permit reduction of the moment M_f (which causes the panel-zone shear in the connection); this introduces design moments for both the main member and the diagonals, and thus requires an integration of member design and connection design.

Figure 9 shows free-body diagrams of the gusset plate at the beam midspan; Figure 10 shows the same at the column. Both figures convert a known set of in-plane forces acting on the gusset plate from connecting members into three forces at the midpoint of the gusset-flange interface: normal force transverse to the member axis, F_N, shear force parallel to the member axis, F_V, and moment in the plane of the web at the face of the member, M_f. The brace forces used for the connection design typically do not include moments, although these could be included in determining the gusset forces.

LOCAL MEMBER FORCES (DERIVATION FOR TWO BRACES)

For simplicity, only two braces are considered in the subsequent derivation: those on "side 1" of the connection. A later section shows the procedure for the inclusion of the effects of an additional gusset on the far side (side 2). These braces may be at equal angles (as is typical for the beam case) or at unequal angles (as happens frequently for the column case

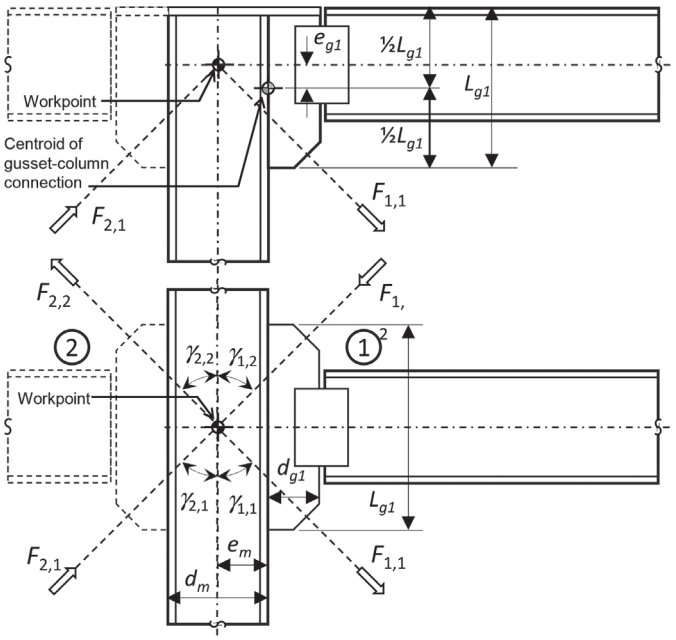

Fig. 7. Column gusset geometry.

and, on occasion, in the beam case). The design equations are presented in general terms applicable to both the beam and the column condition. Minor adjustments to the equations are required for the column case due to the additional forces from the connecting beams; these are noted.

The forces on the gusset-to-flange interface are statically determined. For clarity, brace forces are separated into normal, F_N, and shear, F_V, components. For the column connection, these forces are combined with forces from the beam: V_{Bm}, N_{Bm}, and M_{Bm}, as shown in Figure 10. (For the case of a beam chevron connection, these forces are all zero.) Assuming two braces with forces $F_{1,1}$ and $F_{1,2}$, the shear force is:

$$F_{V1} = F_{1,1}\cos\gamma_{1,1} + F_{1,2}\cos\gamma_{1,2} + V_{Bm1} \quad (1)$$

The normal force is:

$$F_{N1} = F_{1,2}\sin\gamma_{1,2} - F_{1,1}\sin\gamma_{1,1} + N_{Bm1} \quad (2)$$

For the column connection, the collector force N_{Bm1} should be determined from an analysis consistent with brace forces used in the connection design.

In addition to these normal and shear forces, there is a moment (required for static equilibrium). While the moment due to the brace forces is zero at the workpoint, at the flange the moment is:

$$M_{f1} = M_{Ch1} - M_{Bm1} \quad (3)$$

The first term in Equation 3, M_{Ch1}, is the "chevron moment" at the member face. This moment may be conceptualized by considering the forces from the two braces as applied point loads at the locations where their centerlines intersect the member flange. If the brace forces are decomposed into components parallel to and normal to the member axis (Figure 11), the chevron moment can be determined from the normal force components and their eccentricities along the member axis:

$$M_{Ch1} = \left[F_{1,1}\sin(\gamma_{1,1})\right]\left[\frac{e_m}{\tan(\gamma_{1,1})}\right] + \left[F_{1,2}\sin(\gamma_{1,2})\right]\left[\frac{e_m}{\tan(\gamma_{1,2})}\right] \quad (4)$$

which reduces to:

$$M_{Ch1} = F_{V1}e_m \quad (5)$$

The chevron moment is opposed by a moment, M_{FV1}, that corresponds to the parallel components, F_{V1}, multiplied by the eccentricity of the flange from the centerline ($\frac{1}{2}d_m$):

$$M_{FV1} = \left[F_{1,1}\cos(\gamma_{1,1}) + F_{1,2}\cos(\gamma_{1,2})\right]\frac{d_m}{2} = \frac{F_{V1}d_m}{2} \quad (6)$$

which can be simplified to:

$$M_{FV1} = \frac{F_{V1}d_m}{2} \quad (7)$$

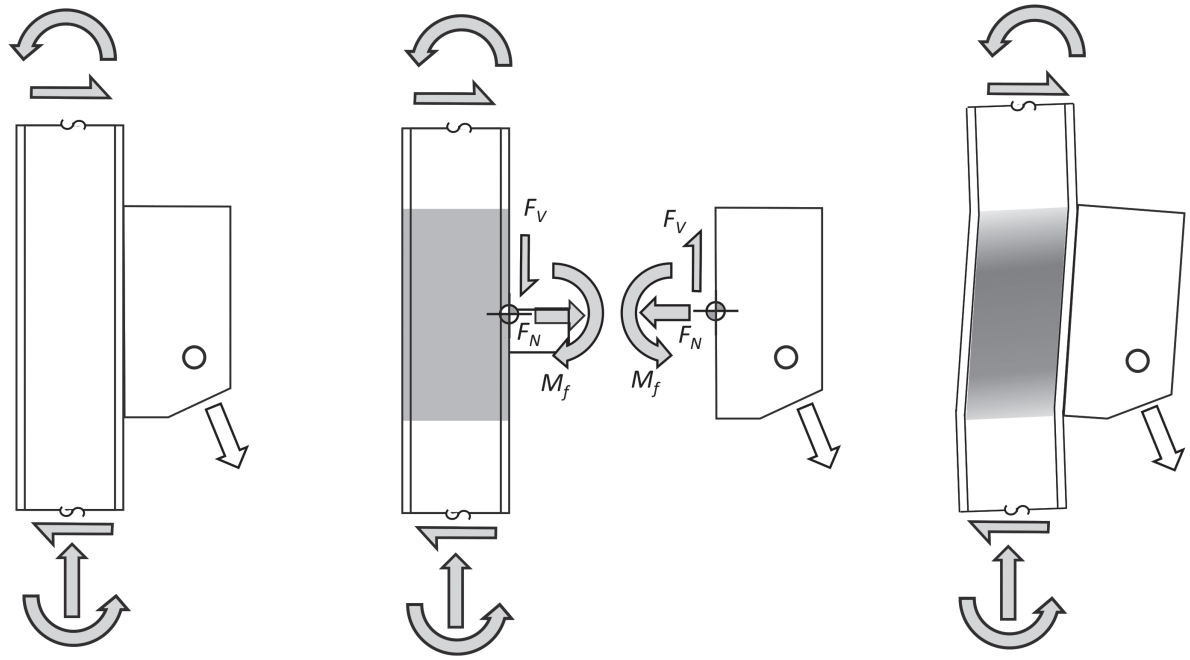

Fig. 8. Free-body diagram of bracket.

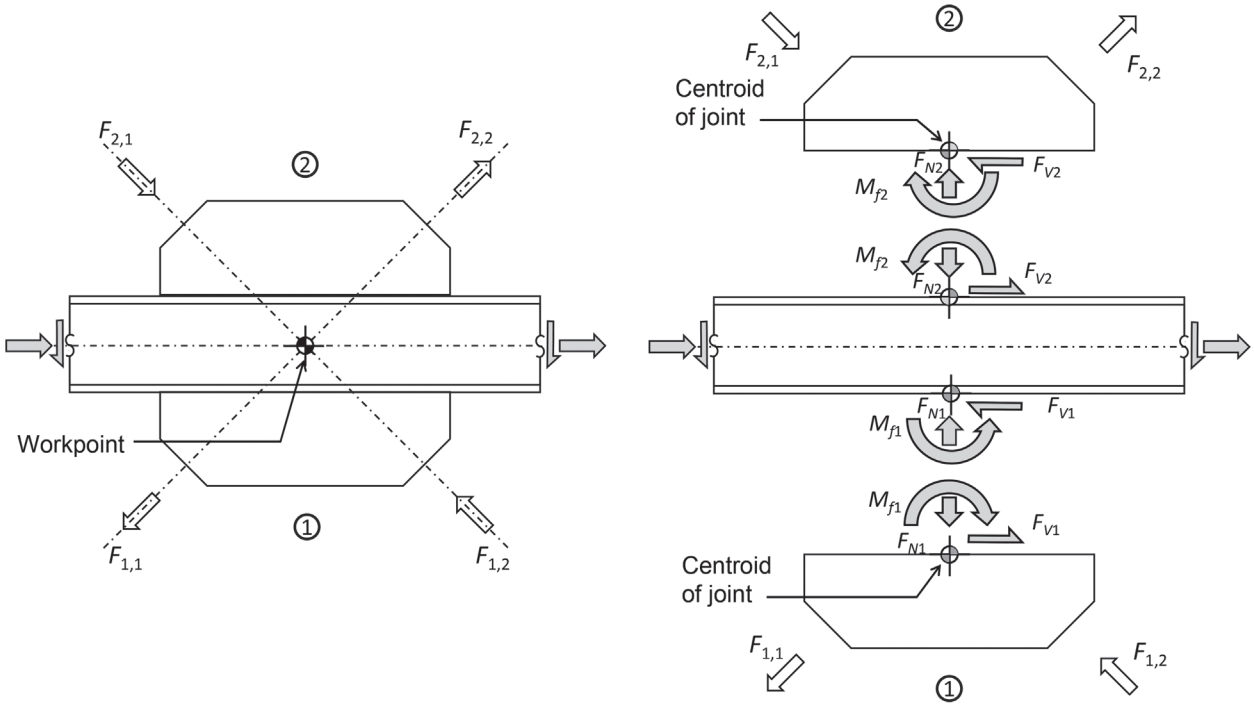

Fig. 9. Force conventions for chevron connection.

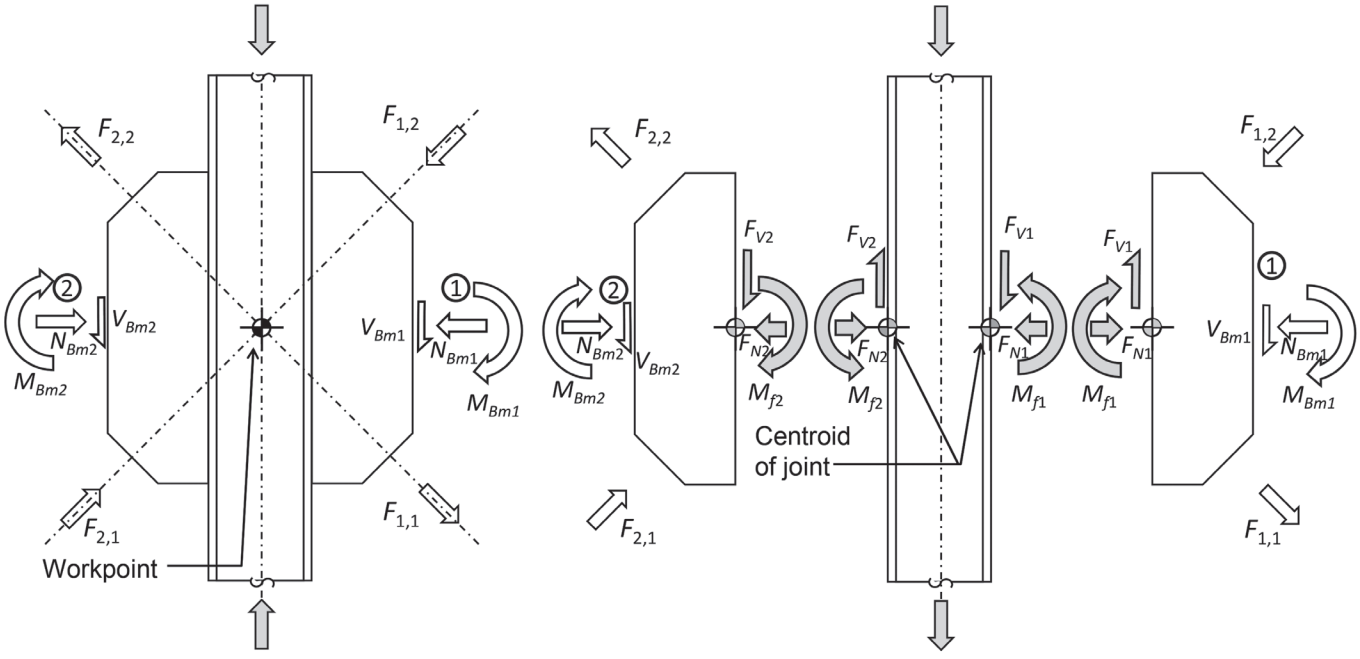

Fig. 10. Force conventions for column connection.

This moment does not affect the gusset or the weld but is necessary for member equilibrium and affects member moment. If the workpoint is at the member centerline (as shown in Figure 9), the distance from the flange to the workpoint, e_m, is:

$$e_m = \frac{d_m}{2} \text{ for the workpoint at the member centerline} \quad (8)$$

If this is the case, the two brace-shear-component-induced moments are equal and opposite ($M_{Ch1} - M_{FV1} = 0$), and there is effectively no moment at the workpoint location on the member centerline due to F_{V1}. If the workpoint is off the member centerline (as shown in Figure 11), the braces induce a moment in the member at the centerline location aligned with the workpoint; this moment causes shear and bending both within and outside of the connection region. Moving the workpoint from the main member centerline toward the gusset reduces the chevron moment while introducing a moment into the main member. In general, such an approach can be economical but requires coordination with member design and building analysis. Similarly, the connection analysis could assign only a portion of this chevron moment to the main member and apply the remainder to the braces. This might reduce the connection demands but would introduce additional design moments into both the main member and the braces, and this member flexure could, in principle, affect the building response to lateral loads. The former approach (modifying the work point) can be integrated with the methods presented in this paper, but the latter approach (assigning counterbalancing moments to the main member and the braces) is separate.

For the column connection, the beam moment, M_{Bm1}, affects the moment at the column flange, M_{f1}. This moment (M_{Bm1}) should be consistent with the brace forces, and the minus sign reflects the direction of forces in Figure 10. Typically, both the beam moment and the brace force are due to the lateral drift. In such cases, the signs are consistent with those shown in Figure 10; when the brace is in compression, the corresponding beam flange is in tension, and vice versa, and thus M_{f1} in Equation 3 is the difference rather than the sum. (The corresponding column shear is additive to the brace forces as discussed later.) Because the effect of the beam moment M_{Bm1} is to reduce the total demand, designers should consider how much of this beneficial effect can be relied on, and a range of this moment could be considered.

For the case of an asymmetric column gusset (such as with only one brace, as shown in the upper diagram of Figure 7), the eccentricity between the gusset midpoint and the beam centerline contributes to the moment:

$$M_{f1} = F_{V1}e_m - M_{Bm1} + F_{N1}e_g \quad (9)$$

A similar adjustment can be made for chevron beams if the gusset midlength and the workpoint are not aligned vertically.

In addition to the "chevron moment," there is a "chevron shear." The chevron shear (V_{Ch1}) is resisted by the gusset and the beam in combination:

$$V_{Ch1} = V_{g1} + V_{mc1} \quad (10)$$

This chevron shear can be determined using static equilibrium on either half segment of the gusset:

$$V_{Ch1} = F_{1,1}\sin\gamma_{1,1} + \frac{1}{2}F_{N1} \quad (11)$$

$$V_{Ch1} = F_{1,2}\sin\gamma_{1,2} - \frac{1}{2}F_{N1} \quad (12)$$

Figure 12 shows a free-body diagrams of beam and gusset segments at the connection, including a transverse section through the beam and gusset showing the sharing of the chevron shear (V_{Ch1}) between the beam shear (V_{mc1}) and the gusset transverse shear (V_{g1}). Note that the location of the centroid of the transverse forces from the gusset segment to the beam flange ($V_{mc1} \pm \frac{1}{2}F_{N1}$) is not specified in the free-body diagrams of the gusset segments; that location may be selected (within certain constraints) in the connection design by the use of a stress distribution model, such as the Elastic Method, the Plastic Method, or the Optimized Plastic Method as described in Section 8 of the AISC *Steel Construction Manual* (2017). Once this location

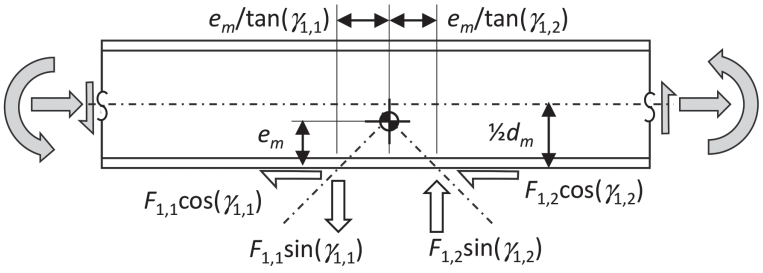

Fig. 11. Brace forces at flange.

is set, the division of V_{Ch1} between V_{mc1} and V_{g1} is statically determined. (Moment at the vertical gusset section is zero, regardless of the stress distribution, for symmetrical conditions with equal brace forces, as shown in the subsequent section, "Gusset Design: Mid-Length Transverse Section.")

The same relationship applies to full-height column gussets. As will be shown in the following sections, the sharing of this chevron shear between the gusset and the beam or column can be controlled by a combination of the gusset dimension selected and the force distribution assumed at the gusset-to-flange interface. In this way, the design methods presented can reduce or eliminate any required web reinforcement.

UNIFORM STRESS METHOD

The Uniform Stress Method is the simplest model for addressing the chevron effect, both for discussion and design purposes. While the treatment of this method here is general, it does not specifically address conditions such as beams with workpoints not at the beam midspan; Fortney and Thornton (2017) provide a more thorough treatment. [The term "Uniform Stress Method" is not employed by Fortney and Thornton. Sabelli and Arber use this term; Hadad and Fortney refer to it as the "Chevron Effects (CE) Method." The term "Uniform Stress Method" has been used in practice and so is used here.]

Fortney and Thornton (2015, 2017) employ the Uniform Stress Method for the transfer of forces over the length of a chevron gusset. In this method, the moment transfer is achieved through two blocks of principal stress in the gusset, each with a length equal to half that of the gusset, as in the "plastic method stress distribution" described in the AISC *Steel Construction Manual*. Figure 13 shows the Uniform Stress Method applied to the column and chevron connections.

Member Shear

Stresses at the member-to-gusset interface are assumed to be distributed uniformly using the full length for the normal and shear forces and a plastic-section-modulus approach for the moment (Fortney and Thornton, 2015). Following this approach, the member shear within the connection region is described by the following equation:

$$V_1(x) = -\frac{2M_{f1}}{L_{g1}} + \frac{4M_{f1}}{L_{g1}^2}|x| + \frac{F_{N1}}{L_{g1}}x + V_M \tag{13}$$

The first two terms are the shear due to the gusset moment, which includes the chevron moment, M_{Ch}, plus any other moment transmitted by the gusset per Equation 3. The third term in the equation is the shear from the unbalanced normal force, and the value at the gusset end ($F_{N1}/2$) is the shear in the member outside of the gusset region for the typical, symmetrical case with $V_M = 0$.

In this equation, x is the distance from the gusset midpoint, as shown in Figure 13. This differs from Fortney and Thornton but is presented in this manner to facilitate combination of forces from gussets of different lengths on opposite flanges of the main member. The member shear is additive for connections with gussets on opposite sides for the typical braced-frame case (with forces as shown in Figures 9 and 10), although the member shear V_M should only be added once. (Hereafter, it is assumed that the member shear V_M is zero in the connection region.)

The maximum shear in the connection region occurs at the gusset midpoint ($x = 0$) and is equal to:

$$V_{mc1} = \frac{2M_{f1}}{L_{g1}} \tag{14}$$

This shear, V_{mc1}, is not equal to the chevron shear, V_{Ch1}, nor to a trigonometric component of either of the brace forces

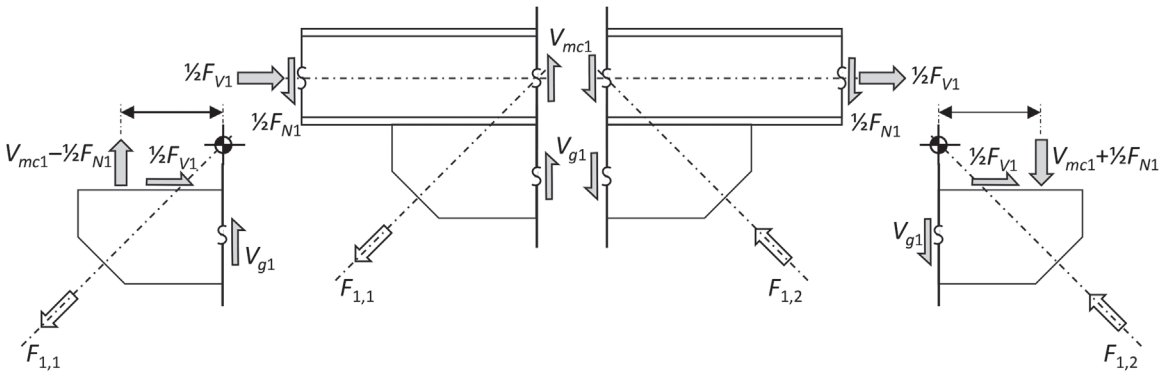

Fig. 12. Transverse section of beam and gusset showing chevron shear.

(e.g., $F_{1,1}\sin\gamma_{1,1}$ or $F_{1,2}\sin\gamma_{1,2}$); it may be greater or smaller than the trigonometric component, depending on the geometry of the connection. The difference between the two is the shear carried by the gusset, V_{g1}, as indicated in Equation 10. The longer the gusset plate, the lower the shear in the main member due to the chevron moment, V_{mc1}, and thus the greater the shear resisted by the gusset, V_{g1}. This is similar to a moment connection in which beam haunches can be used to engage a larger column panel-zone height. In this sense, the gusset plate can be used as external shear reinforcement for the beam, although in this method, it is the length of the gusset that permits it to provide a larger arm for transfer of the chevron moment (and thus reduce the force imposed on the main member) rather than a simple addition of member and gusset shear strength.

Note that this member shear in Equation 14, V_{mc1}, is due only to the force components parallel to the member axis (shear on the connection). The unbalanced normal component does cause shear in the member, but this unbalanced-component shear becomes zero at the workpoint and thus is not considered in conjunction with shear from the balanced component (i.e., the shear from Equation 14). Figure 14 shows a shear diagram for brace-induced shears in a typical pin-end beam consistent with Equation 13.

Note that the maximum member shear occurs at the gusset midpoint (where the member shear neglecting connection effects is zero), and thus the member shear outside of the connection does not affect the maximum shear in the connection region. Concentrated loads within the connection region should be considered by reducing the available shear strength or by engaging the gusset to distribute the load over the gusset length along with the normal force, F_{N1}.

The member shear is the result of both the eccentricity (typically a function of the member depth) and the gusset length. These can be adjusted (within practical bounds) to provide a member that does not require web strengthening. Following this approach, the minimum gusset length to eliminate web strengthening is:

$$L_{g1} \geq \frac{2M_{f1}}{\phi_v V_n} \tag{15}$$

which is equivalent to:

$$L_{g1} \geq \frac{2F_{V1}e_m}{\phi_v V_n} \tag{16}$$

A subsequent section addresses member selection to avoid web reinforcement.

Concentrated Forces

The limit states of web local yielding and web crippling typically can be satisfied without reinforcement at chevron connections, especially those designed using the Uniform Stress Method. These limit states can be evaluated considering two concentrated forces (R_u), each acting on a bearing length of $\frac{1}{2}L_g$:

$$R_{u1} = \frac{F_{N1}}{2} \pm \frac{2M_{f1}}{L_{g1}} \tag{17}$$

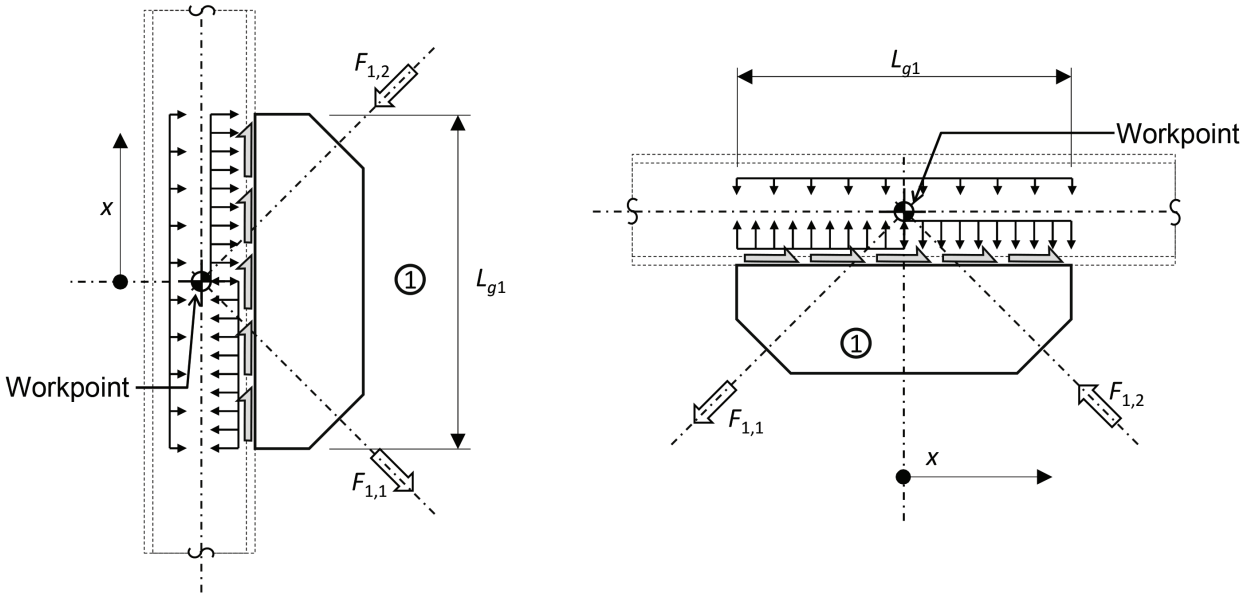

Fig. 13. Uniform Stress Method (after Fortney and Thornton).

Moment

Shear forces in the member have an effect on member moment. While this effect is generally small, Fortney and Thornton (2015) describe conditions in which the beam moment determined using these assumptions (if not considered in design) may necessitate reinforcement using the Uniform Stress Method. Hadad and Fortney (2020) show that in finite element analyses, the beam moments are substantially lower than those calculated using the Uniform Stress Method. While the authors do not propose evaluation of the member moment within the connection region as necessary, examination of the effects that contribute to the moment may aid in understanding of the method.

Beam Moment

In the case of a chevron beam, braces are often considered to be a support point for the beam for wind design. For seismic design of ductile systems, the expected behavior typically entails brace yielding with resulting transverse loading of the beam causing beam shear and bending. [See, for example, AISC *Seismic Provisions* Section F2.3(b).] The beam is evaluated for these forces (adding any gravity loading effects) in combination with the axial force resulting from the components of brace force parallel to the member axis. The combined effect of the moment M_{f1} and the brace force components parallel to the member axis, F_{V1}, produces no shear or flexure outside of the connection region.

For the chevron beam connection, $M_{Bm} = 0$, and thus $M_f = M_{Ch}$. Beam moments within the connection region are described by the following equation:

$$M_1(x) = -\frac{2M_{Ch1}}{L_{g1}}x + \frac{2M_{Ch1}}{{L_{g1}}^2}|x|x - \frac{M_{FV1}}{L_{g1}}x - F_{N1}\left(\frac{L_{beam}}{4} - \frac{L_{g1}}{8} - \frac{x^2}{2L_{g1}}\right) \quad (18)$$

Note that Equation 18 includes more than the integral of the member shear formula (Equation 13). It also includes a distributed moment due to the applied force parallel to the member axis, F_{V1}, at the gusset–flange interface (which, for simplicity, is assumed to be uniformly distributed along the length of the gusset):

$$\frac{M_{FV1}}{L_{g1}} = \frac{F_{V1}e_m}{L_{g1}} \quad (19)$$

Thus:

$$\frac{M_{FV1}}{L_{g1}} = \frac{M_{Ch1}}{L_{g1}} \quad (20)$$

The applied force parallel to the member axis, F_{V1}, thus has two equal and opposing effects: the transverse stress resulting from M_{Ch}, which causes member shear and moment, and the distributed moment corresponding to M_{FV}. These counteracting effects produce zero moment at the ends of the connection region and at the gusset midlength; at other locations, some moment may result based on the differing rates of accumulation over length within the connection region, corresponding to the assumed transverse stress distribution and the assumed distribution of F_{V1} over the gusset length.

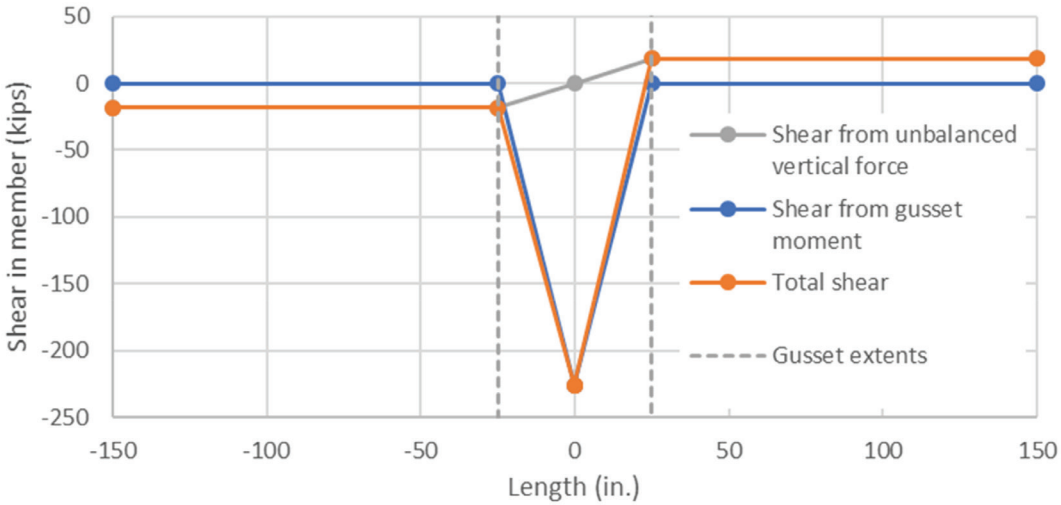

Fig. 14. Brace-induced shears in pin-end beam (Uniform Stress Method).

Equation 18 simplifies to:

$$M_1(x) = -\frac{F_{V1}e_m}{L_{g1}}\left(x - \frac{2}{L_{g1}}x|x|\right) - F_{N1}\left(\frac{L_{beam}}{4} - \frac{L_{g1}}{8} - \frac{x^2}{2L_{g1}}\right) \tag{21}$$

Nonuniform distributions of transfer of the shear force F_V from the gusset to the beam are also admissible, including distributions that minimize or eliminate the local moment effect $M_{Ch}(x) - M_{FV}(x)$. However, the authors have found such approaches unnecessary for demonstrating beam adequacy and, at times, uneconomical for the gusset weld.

A simplified equation can be used to provide a liberal estimate of the maximum brace-induced moment in the beam:

$$M_{max1} \le \left|\frac{F_{V1}e_m}{8}\right| + \left|F_{N1}\left(\frac{L_{beam}}{4} - \frac{L_{g1}}{8}\right) + M_M\right| \tag{22}$$

where M_M is the member moment neglecting brace forces (typically due to gravity). This equation simplifies the determination of moment, providing a liberal upper bound by combining two maxima: the beam moment corresponding to the local shear, $M_{f1}/8$, which occurs at the gusset quarter point, and the midspan moment due to the unbalanced normal force (the second term) and any other beam loading, M_M. (The idealization of the unbalanced normal force as a point load rather than distributed over the gusset length also slightly overestimates the moment.) For the typical braced-frame case (with forces as shown in Figures 9 and 10), the moments from the two gussets are additive, with M_M being added only once.

The first term in Equation 22, $M_{f1}/8$, is a local effect of the connection geometry and is typically small, corresponding to a small eccentricity for the axial force in the beam (which is typically $F_{V1}/4$ at the gusset quarter point).

Column Moment

The column is not required to span to resist the unbalanced brace forces. The column moment in the connection region for the Uniform Stress Method is similar to that from Equation 22:

$$M_{max1} \le \left|\frac{F_{V1}e_m}{8}\right| + |M_M| \tag{23}$$

The effect of any moment M_{Bm} on the member moment is captured in the term M_M, conservatively taken at its full value at the quarter point (where the effect of F_V is at its maximum).

The column moment is typically permitted to be neglected in capacity-design calculations for seismic loads per AISC *Seismic Provisions* D1.4a (AISC, 2016a). For other braced-frame cases this moment is typically very small. The design shear forces outside the connection region are not generally large, especially for frames with pin-ended beams.

CONCENTRATED STRESS METHOD

In the preceding discussion, the Uniform Stress Method stress distribution was assumed to determine the member forces in the connection region. The calculated member shear may be reduced by selecting a more favorable distribution. The Concentrated Stress Method maximizes the moment arm within a given gusset length and thus minimizes the corresponding force caused by the moment. This method is based on the Optimized Plastic Method (AISC, 2017), modified to optimize only for moment resistance (rather than both moment and normal force) and to allow for incorporation of design limits based on both gusset yield and member limit states.

In the Concentrated Stress Method, the moment M_{f1} is assumed to be transferred at the ends of the gusset over lengths z_1. The remaining segment in the middle of the gusset does not participate in transmitting the flexure; it is assumed to resist the unbalanced force F_{N1}. Figure 15 shows this stress distribution.

Member Shear and Minimum Gusset Length

The Concentrated Stress Method converts the moment M_{f1} into a normal force couple R_{z1} with a moment arm of e_{z1}. This normal force R_{z1} is distributed over a length z_1. The values of R_{z1} and e_{z1} are determined such that R_{z1} does not exceed the force that would cause shear yielding of the member.

Figure 16 shows a shear diagram corresponding to this stress distribution for a chevron connection. Note that the maximum beam shear in the Concentrated Stress Method does not occur at the beam midpoint (as it does for the Uniform Stress Method), and thus the beam shear outside of the connection affects the maximum shear within the connection region.

The moment arm e_{z1} is:

$$e_{z1} = L_{g1} - z_1 \tag{24}$$

The normal force from the moment transfer is thus:

$$R_{z1} = \frac{M_{f1}}{e_{z1}} \tag{25}$$

$$R_{z1} = \frac{M_{f1}}{L_{g1} - z_1} \tag{26}$$

This normal force causes shear in the member. For beams, the maximum shear is a combination of the shear due to the unbalanced force and the shear due to delivery of

the chevron moment. The maximum shear is given by the following equation:

$$V_{mc1} = V_{ma1} + R_{z1} \tag{27}$$

The shear outside of the connection region, V_{ma1}, is due to net normal force, F_{N1}, and the member shear from gravity or other sources, V_M:

$$V_{ma1} = \frac{1}{2} F_{N1} + V_M \tag{28}$$

The shear V_M is typically zero adjacent to (and within) the connection region for beams.

If the gusset is long enough, the total connection shear V_{mc} may be set less than or equal to the design shear strength of the member in order to preclude the need for shear reinforcement. For a given gusset length, the maximum moment transfer can be achieved by the highest concentration of stress at the ends. For a minimum gusset length, stiffeners at the gusset edges may be used to create a moment arm

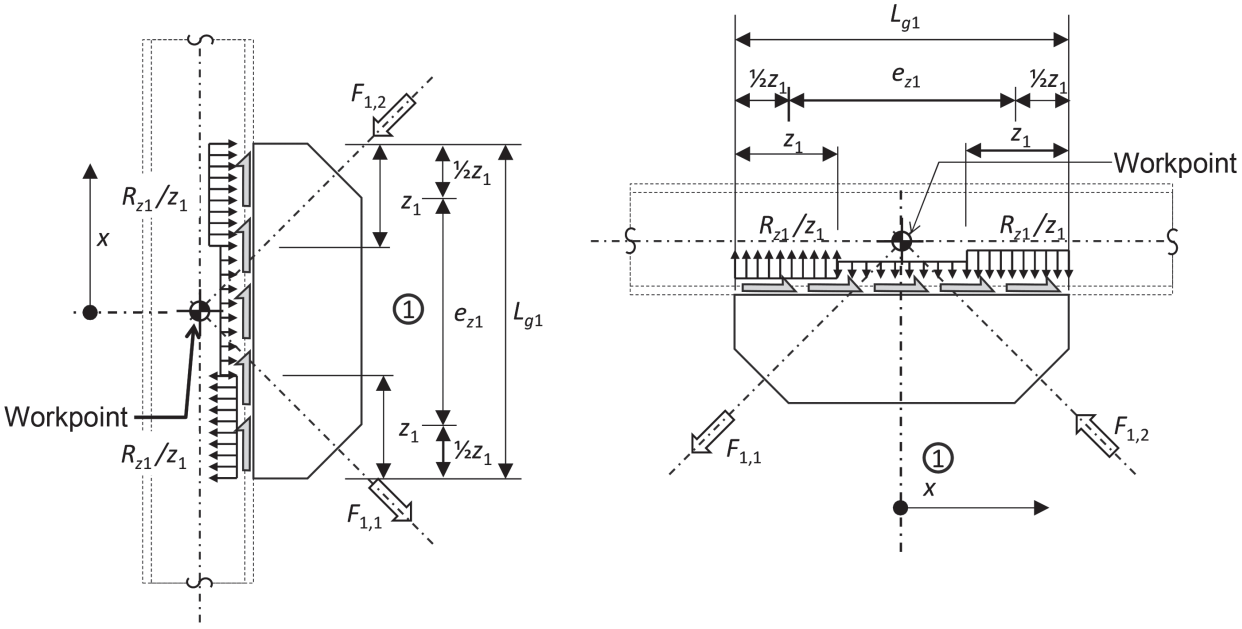

Fig. 15. Stress distribution for the Concentrated Stress Method.

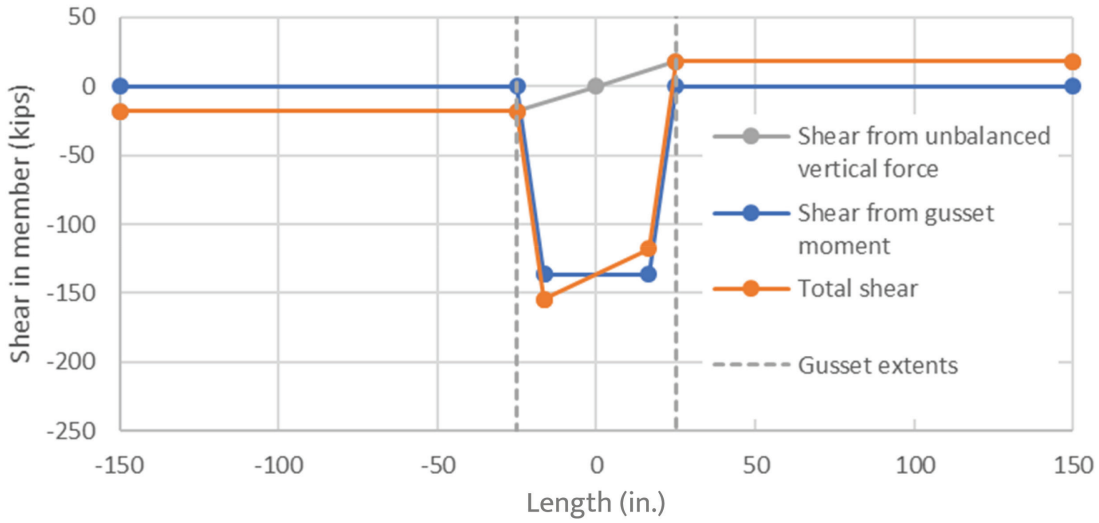

Fig. 16. Brace-induced shear in pin-end beam with Concentrated Stress Method.

equal to the gusset length L_{g1}, similar to a moment connection in which beam flanges deliver moment to the face of a column. For the more typical chevron-moment transfer via the gusset plate, the concentrated stress may be limited by web local yielding, web crippling, or the gusset yielding.

If the gusset length is minimized (without stiffeners), the concentrated stress will be maximized such that the full member shear strength is utilized. Unlike the Uniform Stress Method, in the Concentrated Stress Method the maximum member shear is maintained over a significant portion of the connection length, and thus (for beams) occurs at locations that also have shear induced by the unbalanced normal force from braces. Considering that some of the shear strength is utilized in resisting this unbalanced force, the remaining member shear strength that can be utilized for the moment transfer is:

$$V_{ef1} = \phi_v V_n - V_{ma1} \tag{29}$$

For designs with a gusset on the opposite flange, both the design shear strength (ϕV_n) and the net shear outside the connection ($V_{ma1} - V_{ma2}$) can be apportioned between the two gusset designs. This is addressed in a later section.

The Concentrated Stress Method is derived such that the maximum shear from Equation 26 does not exceed the effective shear strength from Equation 29:

$$R_{z1} \le V_{ef1} \tag{30}$$

The minimum gusset length possible corresponds to the use of stiffeners (flanges) to transfer the moment M_{f1}. Thus as z_1 approaches zero, Equation 26 (combined with Equation 30) gives the minimum gusset length dimension:

$$L_{g1} = \frac{M_{f1}}{V_{ef1}} \ for \ z_1 = 0 \tag{31}$$

Without such stiffeners, there is a finite length of gusset z_1 over which the force R_{z1} is transferred to the beam. The minimum length z_1 may be governed by the limit states of web local yielding, web crippling, or yielding of the gusset. For web local yielding, AISC *Specification* Equation J10-2 (AISC, 2016b) can be rearranged to solve for the minimum bearing length z_1:

$$z_1 \ge \frac{R_{z1}}{\phi_w w F_y t_w} - 5k \tag{32}$$

The corresponding minimum gusset length based on the web local yielding limit state is:

$$L_{g1} \ge e_{z1} + z_1 \tag{33}$$

Combining Equations 24, 32, and 33:

$$L_{g1} \ge \frac{M_{f1}}{R_{z1}} + \frac{R_{z1}}{\phi_w F_y t_w} - 5k \tag{34}$$

This length is minimized by taking the maximum normal force R_{z1} that the member can resist based on its effective shear strength per Equation 30.

Considering combined shear and tension in the gusset, the minimum gusset thickness corresponding to the minimum length selected using Equation 34 and the maximum normal force R_{z1} (equal to V_{ef1}) is determined using the von Mises yield criterion, with shear stress over the full gusset length and the moment delivered by a force couple.

A gusset that satisfies this criterion is required:

$$t_{g1} \ge \sqrt{\left(\frac{F_{V1}}{\phi_v 0.6 F_y L_{g1}}\right)^2 + \left(\frac{R_{z1}}{\phi_t F_y (L_{g1} - e_{z1})}\right)^2} \tag{35}$$

which is equivalent to:

$$t_{g1} \ge \sqrt{\left(\frac{F_{V1}}{\phi_v 0.6 F_y L_{g1}}\right)^2 + \left[\frac{R_{z1}}{\phi_t F_y \left(L_{g1} - \frac{M_{f1}}{R_{z1}}\right)}\right]^2} \tag{36}$$

The center zone may be similarly examined, although generally this zone is much less stressed:

$$t_{g1} \ge \sqrt{\left(\frac{F_{V1}}{\phi_v 0.6 F_y L_{g1}}\right)^2 + \left(\frac{F_{N1}}{\phi_t F_y (L_{g1} - 2z_1)}\right)^2} \tag{37}$$

which is equivalent to:

$$t_{g1} \ge \sqrt{\left(\frac{F_{V1}}{\phi_v 0.6 F_y L_{g1}}\right)^2 + \left[\frac{F_{N1}}{\phi_t F_y \left(\frac{2M_{f1}}{R_{z1}} - L_{g1}\right)}\right]^2} \tag{38}$$

If the required gusset thickness is excessive, a longer gusset may be employed. The gusset length required for a given gusset thickness is the root of a fourth-power polynomial, for which various solution methods are available, including trial-and-error and computer solvers. A closed-form solution may also be derived using Ferrari's formula (Euler, 1765). A simple approximate formula can be obtained, however, if the shear, F_{V1}, is neglected and R_{z1} is set equal to V_{ef1}:

$$L_{g1} > \frac{M_{f1}}{V_{ef1}} + \frac{V_{ef1}}{t_{g1} \phi_t F_y} \tag{39}$$

As in the design example, a length slightly greater than that indicated by Equation 39 is generally satisfactory.

Because of the complexity of the equations for web crippling, that limit state is not integrated into the equations for minimum gusset length but may be evaluated after the gusset length is determined, as shown in the subsequent section.

Gussets Longer than the Minimum Length

In many cases, the gusset length will exceed the minimum from Equation 34, due to design considerations such as the required gusset thickness or the brace-to-gusset attachment. For gussets longer than the minimum, the designer has some flexibility in selecting a stress distribution that transfers the moment. Maximizing the length z decreases the moment arm and thus increases the force to be resisted; it also leaves less weld length for the forces that are resisted in the center zone. The authors have found that the total weld volume tends to be minimized by minimizing the length z_1 for optimized weld lengths and sizes. However, in many cases, the weld size in the center zone is controlled by a minimum weld size, or a proportioning requirement to ensure deformation compatibility is used to size the center-zone weld or the minimum length for z_1; in such cases, maximizing the length z_1 may be more economical.

The minimum length z_1 is determined considering web local yielding, web crippling, and gusset yielding, considering the normal force R_{z1} acting over the length z_1 (and combined with a shearing force for the gusset evaluation). The force R_{z1} corresponding to the length z_1 is determined by Equation 26 and is bounded by Equation 30.

Considering web local yielding, the minimum length z_1 is:

$$z_1 \geq \frac{L_{g1}}{2} - \sqrt{\frac{{L_{g1}}^2}{4} - \frac{M_{f1}}{\phi_w F_y t_w}} - 5k \tag{40}$$

The von Mises yield criterion is used to determine the minimum length z_1 that, for the design loads and a given gusset thickness and length, will result in effective stresses at the yield limit in the gusset. The shear stress is due to F_{V1} and the normal stress is due to the moment M_{f1}. The thickness should satisfy Equation 36. The length z_1 corresponding to the gusset length and thickness selected is obtained by combining Equations 24, 26, and 36:

$$z_1 \geq \frac{L_{g1}}{2} - \sqrt{\frac{{L_{g1}}^2}{4} - \frac{M_{f1}/\phi_t}{\sqrt{\left(F_y t_g\right)^2 - \left(\frac{F_{V1}}{\phi_v 0.6 L_{g1}}\right)^2}}} \tag{41}$$

Considering web crippling, the minimum length z_1 can be determined by rearranging AISC *Specification* Equation J10-4:

$$z_1 \geq \left[\frac{R_{z1}}{\phi_n 0.80 t_w^2}\sqrt{\frac{t_w}{E F_y t_f}} - 1\right]\left(\frac{d_m}{3}\right)\left(\frac{t_f}{t_w}\right)^{1.5} \tag{42}$$

Due to the number of terms of Equation 42, it is convenient to use the maximum value of $R_{z1} = V_{ef1}$ per Equation 30 rather than solving for z_1 using Equations 26 and 42. Alternatively, web crippling can be evaluated using R_{z1} corresponding to the larger of the values from Equations 40 and 41.

The minimum value of z_1 is the largest of the values from Equations 40, 41, and 42. Larger values of z_1 may be used up to a maximum value of z_1 limited by the minimum moment arm corresponding to the maximum transverse force:

$$z_1 \leq L_{g1} - \frac{M_{f1}}{V_{ef}} \tag{43}$$

Above this value of z_1, the length of the moment arm e_z is insufficient and the transverse force required to transmit the moment will exceed V_{ef}. If this maximum value is negative the gusset is too short to transmit the moment regardless of how concentrated the force delivery can be.

In principle, the maximum value of z_1 may also be limited by stresses in the center region. Use of the additional bearing length of $5k$ (as opposed to $2.5k$) in Equation 40 distributes some of the force R_{z1} into the center region. For cases with high unbalanced load (or very small dimension e_z), $2.5k$ may be used in Equation 40, or the following evaluation can be made based on the total transverse force $R_{z1} + F_{N1}$ acting on a length $L_{g1} - z_1$:

$$z_1 \leq L_{g1} - \frac{R_{z1} + F_{N1}}{\phi_w F_y t_w} + 5k \tag{44}$$

Similarly, if the normal force F_{N1} is large (or the center zone is very short), the gusset stress in the center region should also be considered. Using the von Misses yield criterion gives this maximum:

$$z_1 \leq \frac{1}{2}\left[L_{g1} - \frac{F_{N1}/\phi_t F_y t_{g1}}{\sqrt{1 - \left(\frac{F_{V1}}{\phi_v 0.6 F_y t_{g1} L_{g1}}\right)^2}}\right] \tag{45}$$

Concentrated Stress Method Validation

Richards et al. (2018) analyzed a number of braced-frame beams using finite element models and compared internal forces with those obtained from the Uniform Stress Method and the Concentrated Stress Method (as presented by Sabelli and Arber, 2017). Figure 17 shows the results of one such analysis (from Figure 3.32 from Richards et al.). The finite element analysis results (FE) are shown along with the shears determined using the Uniform Stress Method (USM) and the Concentrated Stress Method (CSM, using the modified method as presented in this paper); the beam shear strength, ϕV_n, is also indicated. The values of maximum shear are reasonably consistent between the finite element analysis and the Concentrated Stress Method for this example, and while the total shear in the finite element model is less than the beam shear capacity, the finite element analysis indicated local yielding in the web.

Nevertheless, the point of maximum shear is not identical between the finite element analysis and the Concentrated Stress Method, indicating that the Concentrated Stress Method, while useful for design, is not a perfect representation of the internal stresses.

It should be noted that both Richards et al. (2018) and Hadad and Fortney (2020) found that the Uniform Stress Method is generally representative of the beam shear at levels of loading that do not result in web shear yielding. At higher levels of loading, the work of Richards et al. (2018) indicates adequate performance of gussets meeting the minimum required length for the Concentrated Stress Method and exceeding the length required for the Uniform Stress Method. Additional comparisons of finite-element analyses from Richards et al. with the two design models are presented in Sabelli et al. (2020).

Moment

Shear, such as shown in the three analyses represented in Figure 17, implies moment. The authors do not propose evaluation of the member moment within the connection region as necessary but present the equations for moment to facilitate understanding of the Concentrated Stress Method. Hadad and Fortney (2020) show that in finite element analyses, the beam moments are substantially lower than those calculated using the Uniform Stress Method.

Beam Moment

The beam moment is the combination of the integral of the beam shear and the distributed moment M_{FV} (Equation 19).

The beam shear in the center region is:

$$V_1(x) = -R_{z1} + \frac{F_{N1}}{L_{g1}}x \qquad \text{for } |x| \le L_{g1}/2 - z_1 \tag{46}$$

In the z_1 region, the beam shear is:

$$V_1(x) = -R_{z1}\left(\frac{L_{g1}}{2z_1} - \frac{|x|}{z_1}\right) + \frac{F_{N1}}{2}\frac{|x|}{x} \tag{47}$$
$$\text{for } |x| \ge L_{g1}/2 - z_1$$

Similar to the Uniform Stress Method, the distributed moment M_{FV} may be assumed to be transferred over the length L_{g1} using Equation 19. The brace-induced moment in the beam is:

$$M_1(x) = -R_{z1}x + \frac{M_{FV1}}{L_{g1}}x - F_{N1}\left(\frac{L_{beam}}{4} - \frac{L_{g1}}{8} - \frac{x^2}{2L_{g1}}\right) \tag{48}$$
$$\text{for } |x| \le L_{g1}/2 - z_1$$

Similar to the Uniform Stress Method, the two equal and opposing effects of the applied force parallel to the member axis, F_{V1}, are included in Equation 48: the transverse stress resulting from M_{Ch}, which causes member shear in addition to moment, and the distributed moment corresponding to M_{FV}, which does not affect the shear. The shape of the shear diagram in the Concentrated Stress Method results in a somewhat smaller moment within the connection region than that corresponding to the Uniform Stress Method.

A liberal estimate may be made by computing the connection-induced moment and combining with the mid-span moment due to overall beam flexure:

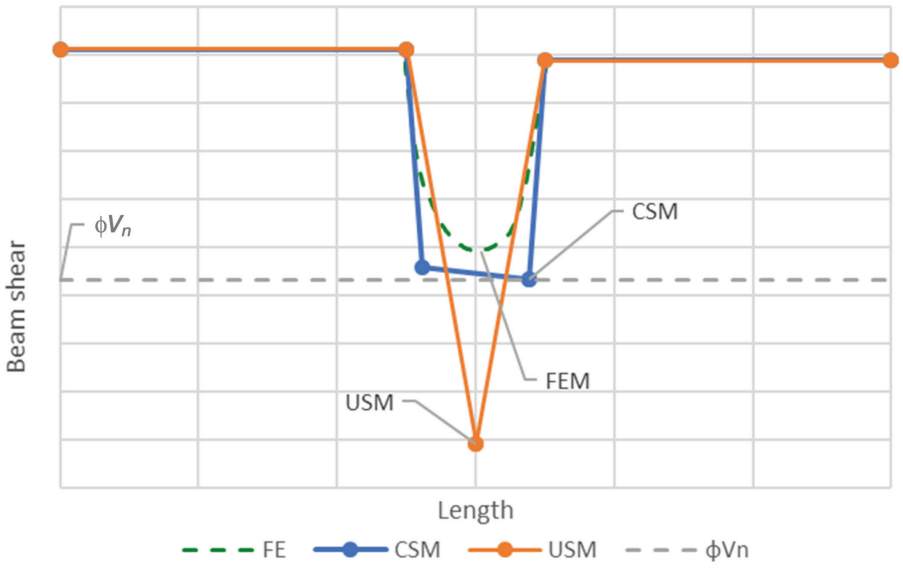

Fig. 17. Concentrated Stress Method (CSM) and Uniform Stress Method (USM) analysis of beam from Richards et al. (2018).

$$M_{max1} \le \frac{|M_{Ch1}|}{2}\left[\frac{z_1}{L_{g1}} - \left(\frac{z_1}{L_{g1}}\right)^2\right] + F_{N1}\left(\frac{L_{beam}}{4} - \frac{L_{g1}}{8}\right) + M_M \tag{49}$$

The connection-induced moment due to M_{Ch} never exceeds $M_{Ch}/8$ (the value for $z_1 = L_{g1}/2$, which corresponds to the Uniform Stress Method distribution). The moment is additive with the moment from gusset 2 for the typical braced-frame case.

Column Moment

Similar methods can be applied to calculate moment in the column within the connection region. Column moments due to frame behavior, which reverse over the connection depth, are typically additive to the effect of M_{Ch}.

$$M_{max1} \le \frac{M_{Ch1}}{2}\left[\frac{z_1}{L_{g1}} - \left(\frac{z_1}{L_{g1}}\right)^2\right] + M_M \tag{50}$$

The effect of any moment M_{Bm} on the member moment is captured in the term M_M, conservatively taken at its full value. Similar to the beam moment, the column moment due to the chevron effect tends to be small.

COMBINATION OF FORCES FOR TWO GUSSET PLATES

The member forces derived are for braces on one side with opposite forces (one brace in tension and the other in compression). These forces may be combined with gravity-induced forces and with shear due to flexural restraint for frames with moment connections. While the diagrams show the left brace in tension and the right brace in compression, forces corresponding to the opposite case are easily determined by using negative values for the brace forces.

For a configuration with braces on both sides of the member (such as a two-story X-configuration in a beam), brace-induced shears and moments will be additive for the typical case in which the story shears are in the same direction. The effective web shear resistance may be apportioned between the two gussets, considering the relative magnitudes of their moments, M_f, to permit independent design of the two gussets:

$$V_{ef1} = \frac{M_{f1}}{M_{Tot}} V_{efTot} \tag{51}$$

and

$$V_{ef2} = \frac{M_{f2}}{M_{Tot}} V_{efTot} \tag{52}$$

where

$$M_{Tot} = M_{f1} + M_{f2} \tag{53}$$

Other methods of apportionment are admissible, but this method allows for design of the gusset connections based on member forces established prior to gusset design and without additional interdependence.

Uniform Stress Method

In the Uniform Stress Method, the full member shear strength generally may be utilized:

$$V_{efTot} = \phi_v V_n \tag{54}$$

Gusset plates may be of different lengths, but for simplicity, they may be set to be equal. If equal-length gussets are used ($L_{g1} = L_{g2}$), Equation 15 for the minimum gusset-plate length to preclude the need for reinforcement can be modified thus:

$$L_g \ge \frac{2M_{Tot}}{V_{efTot}} \tag{55}$$

Concentrated Stress Method

In the Concentrated Stress Method, the effective beam shear strength is reduced:

$$V_{efTot} = \phi_v V_n - \left|\frac{F_{N1}}{2} - \frac{F_{N2}}{2}\right| - |V_M| \tag{56}$$

If equal-length gussets are used, Equation 34 for the minimum gusset-plate length to preclude the need for reinforcement can be modified thus:

$$L_g \ge \frac{M_{Tot}}{V_{efTot}} + \frac{V_{efTot}}{\phi_w F_y t_w} - 5k \tag{57}$$

Similarly, Equation 39 based on gusset yielding can be modified thus:

$$L_{g1} > \frac{M_{Tot}}{V_{efTot}} + \frac{V_{efTot}}{t_{g1}\phi_t F_y} \tag{58}$$

MEMBER SELECTION

The procedures described earlier allow for the design of a connection based on design forces and the strength of a member already selected. Economy in steel construction can often be achieved by consideration of connection requirements in member selection. Equations for required beam strength, rather than required gusset length, can be derived from the methods presented. Fortney and Thornton (2015) suggest a preliminary assumption of a gusset length of one-sixth of the beam span for chevron connections; this value can be used to facilitate member selection.

The chevron shear at the connection is due mainly to the chevron moment, M_{ch}, which is proportional to the eccentricity, e_m, typically half the member depth. Selection of a shallower member reduces the eccentricity and thus reduces the chevron shear. Because the shear capacity is also proportional to the depth, the member depth appears in both the demand and capacity terms, and the required web thickness is not a function of member depth.

Uniform Stress Method

Using the Uniform Stress Method equation for minimum gusset length for a given member strength (Equation 15), the minimum shear strength is

$$\phi_v V_n = \phi_v 0.6 F_y d_m t_w \tag{59}$$

$$\phi_v V_n \geq \frac{2M_{f1}}{L_{g1}} + \frac{2M_{f2}}{L_{g2}} \tag{60}$$

$$\phi_v V_n \geq \frac{F_{V1} d_m}{L_{g1}} + \frac{F_{V2} d_m}{L_{g2}} \tag{61}$$

Note that the member depth appears both in the demand, M_{f1}, and in the resistance, ϕV_n, and thus cancels out in Equation 62 for the minimum member web thickness:

$$t_w \geq \frac{F_{V1}/L_{g1} + F_{V2}/L_{g2}}{\phi_v 0.6 F_y} \tag{62}$$

For beams or columns with small moments due to unbalanced normal forces, a shallow member meeting this requirement may be economical. Note that the optimal gusset length may be a function of member depth.

Concentrated Stress Method

Use of a member with web thickness less than that required by Equation 62 necessitates either reinforcement of the web or use of a greater moment arm to deliver the moment M_{f1} than is assumed in the Uniform Stress Method (such as e_{z1} in the Concentrated Stress Method). There is not a corresponding simple equation for minimum web thickness using the Concentrated Stress Method. However, the minimum gusset length based on beam shear strength with $z_1 = 0$ (Equation 31) represents a limiting value. This minimum gusset length corresponds to a moment arm e_{z1} equal to L_{g1} (rather than $\frac{1}{2}L_{g1}$, as corresponds to the Uniform Stress Method and Equation 62), and thus, if there are no other member shear demands to consider, the required web thickness for this limiting case is half of that from Equation 62. A web thickness of 60% to 75% of that given by Equation 62 (based on an assumed gusset length) generally permits use of the Concentrated Stress Method without the need for web reinforcement, albeit with possible moderate adjustment in gusset length. (Use of 75% of the value from Equation 62 requires $e_{z1} \sim \frac{2}{3} L_{g1}$; use of 60% requires $e_{z1} \sim \frac{5}{6} L_{g1}$.)

GUSSET AND WELD DESIGN

The stress distributions assumed in the Uniform Stress Method and the Concentrated Stress Method impose different demands on gusset plates and welds. The design of those elements should be compatible with each other (and with the checks on member local limit states, such as web local yielding, web crippling, and panel-zone shear), or the connection may not be able to resist the applied forces. For example, if the design for local limit states is based on the Uniform Stress Method, but the gusset thickness is sized using the optimized plastic stress method (which is implicit in the interaction Equation 9-1 in the AISC *Steel Construction Manual*), the member may be subject to a combination of web local yielding and gusset plate yielding prior to developing the required strength. It is recommended that the method used for member local limit states be carried through the design of the gusset and the weld.

Gusset Design: Section Parallel to Member Axis

Uniform Stress Method

For the Uniform Stress Method, the gusset section at the interface with the flange can be evaluated using an interaction method such as the von Mises yield criterion and solving for the required thickness:

$$t_g \geq \sqrt{\left(\frac{|4M_{f1}|}{\phi_t F_y L_{g1}^2} + \frac{|F_{N1}|}{\phi_t F_y L_{g1}}\right)^2 + \left(\frac{F_{V1}}{\phi_v 0.6 F_y L_{g1}}\right)^2} \tag{63}$$

Concentrated Stress Method

For the Concentrated Stress Method, the gusset section at the interface with the flange is implicitly designed by use of a length z conforming to Equations 36 and 38.

Gusset Design: Mid-Length Transverse Section

Statics require that certain forces be transferred across the midpoint of the gusset. Figure 18 shows free-body diagrams of half of a gusset for both the Uniform Stress Method (a) and the Concentrated Stress Method (b).

The normal force on the gusset transverse section (i.e., the force parallel to the member axis) for both models is:

$$N_{g1} = \frac{1}{2} F_{V1} - F_{1,1} \cos \gamma_{1,1} \tag{64}$$

which is equivalent to:

$$N_{g1} = \frac{1}{2}(F_{1,2}\cos\gamma_{1,1} - F_{1,1}\cos\gamma_{1,2}) \quad (65)$$

Uniform Stress Method

The shear on this gusset section transverse to member axis (for the Uniform Stress Method) is:

$$V_{g1} = F_{1,1}\sin\gamma_{1,1} - \frac{2M_{f1}}{L_{g1}} + \frac{F_{N1}}{2} \quad (66)$$

The gusset moment (for the Uniform Stress Method) is:

$$M_{g1} = \left(\frac{2M_{f1}}{L_{g1}} - \frac{F_{N1}}{2}\right)\frac{L_{g1}}{4} + N_{g1}\left(e_m + \frac{d_{g1}}{2}\right) - \frac{F_{V1}}{2}e_m \quad (67)$$

which simplifies to:

$$M_{g1} = N_{g1}\left(e_m + \frac{d_{g1}}{2}\right) - \frac{F_{N1}L_{g1}}{8} \quad (68)$$

Concentrated Stress Method

The gusset shear transverse to member (for the Concentrated Stress Method) is:

$$V_{g1} = F_{1,1}\sin\gamma_{1,1} - R_{z1} + \frac{F_{N1}}{2} \quad (69)$$

The gusset moment (for the Concentrated Stress Method) is:

$$M_{g1} = R_{z1}\left(\frac{L_{g1}}{2} - \frac{z_1}{2}\right) - \frac{F_{N1}}{2}\left(\frac{L_{g1}}{4} - \frac{z_1}{2}\right) + N_{g1}\left(e_m + \frac{d_{g1}}{2}\right) - \frac{F_{V1}}{2}e_m \quad (70)$$

which simplifies to:

$$M_{g1} = N_{g1}\left(e_m + \frac{d_{g1}}{2}\right) - \frac{F_{N1}L_{g1}}{8} + \frac{F_{N1}z_1}{4} \quad (71)$$

Note that the terms related to M_{f1} and F_{V1} cancel out in both Equations 68 and 71. Thus, the gusset moment is only due to the unequal brace force components transverse to the member axis (resulting in an unbalanced transverse force F_{N1}) and to unequal brace force components parallel to the member axis (resulting in a force transfer N_{g1} from one half of the gusset to the other), with those two effects offsetting each other.

The gusset should be evaluated for the interaction of these shear, normal, and moment forces. This may be done using von Mises yield criteria or other methods as discussed in the AISC *Steel Construction Manual* (AISC, 2017).

Gusset Design: Diagonal Section (Concentrated Stress Method)

Brace-to-gusset connections are typically evaluated for the limit state of block shear without consideration of the subsequent load path through the gusset. This may not

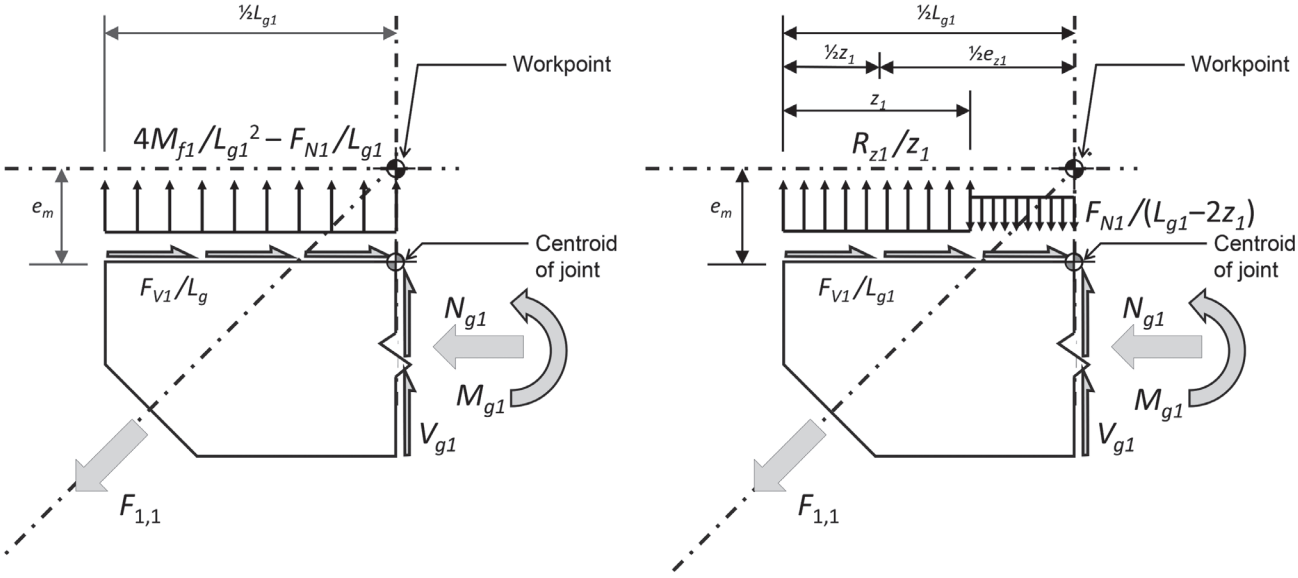

(a) Uniform Stress Method *(b) Concentrated Stress Method*

Fig. 18. Free-body diagrams of half gusset.

present any significant inconsistency for the Uniform Stress Method, which assumes a uniform stress over each half of the gusset, but may for the Concentrated Stress Method, in which high stresses are assumed at the gusset zones z_1. In order to ensure that the gusset has sufficient strength to transfer the force R_{z1} to the region z_1 in the gusset-to-beam connection, the gusset should be evaluated along a diagonal section, as shown in Figure 19. That section is aligned with the outside shear area used in the block-shear calculation and projected to the beam–gusset interface.

The intersection of the diagonal section with the gusset edge occurs at a point defined by the dimension X_{crit}:

$$X_{crit} = \frac{L_g}{2} - \frac{e_m}{\tan\gamma} - \frac{W}{2\sin\gamma} \tag{72}$$

thus,

$$X_{crit} = \frac{L_g}{2} - \frac{d_m\cos\gamma + W}{2\sin\gamma} \tag{73}$$

The length of the section is determined using the dimensions indicated in Figure 19:

$$\frac{D_{clip}}{\sin\gamma} = X_{crit}\tan\gamma - (d_g - Y_{clip}) \tag{74}$$

$$D_{crit} = \frac{X_{crit}}{\cos\gamma} - D_{clip} \tag{75}$$

$$D_{crit} = X_{crit}\cos\gamma + (d_g - Y_{clip})\sin\gamma \tag{76}$$

Note that this length is somewhat greater than the length of one of the shear areas used for the block-shear rupture check in the gusset plate. In some cases, a simplified check with that portion of the block-shear area suffices.

The forces acting to the left of that section are:

$$F_{X\,crit} = \frac{X_{crit}}{L_g} F_V \tag{77}$$

If X_{crit} is less than or equal to z:

$$F_{Ycrit} = \frac{X_{crit}}{z} R_z \tag{78}$$

$$e_{crit} = \frac{X_{crit}}{2} \tag{79}$$

$$M_{crit} = F_{Ycrit}\left(e_{crit} - \frac{D_{crit}\cos\gamma}{2}\right) + F_{Xcrit}\frac{D_{crit}\sin\gamma}{2} \tag{80}$$

If X_{crit} is greater than z_1:

$$F_{Ycrit} = R_z + F_N\frac{X_{crit} - z}{L_g - 2z} \tag{81}$$

Note that on one side of the gusset, the two terms of Equation 81 will be additive; that is the more critical condition.

$$e_{crit} = \frac{R_z(X_{crit} - z/2) + F_N\dfrac{(X_{crit} - z)^2}{2(L_g - 2z)}}{F_{Ycrit}} \tag{82}$$

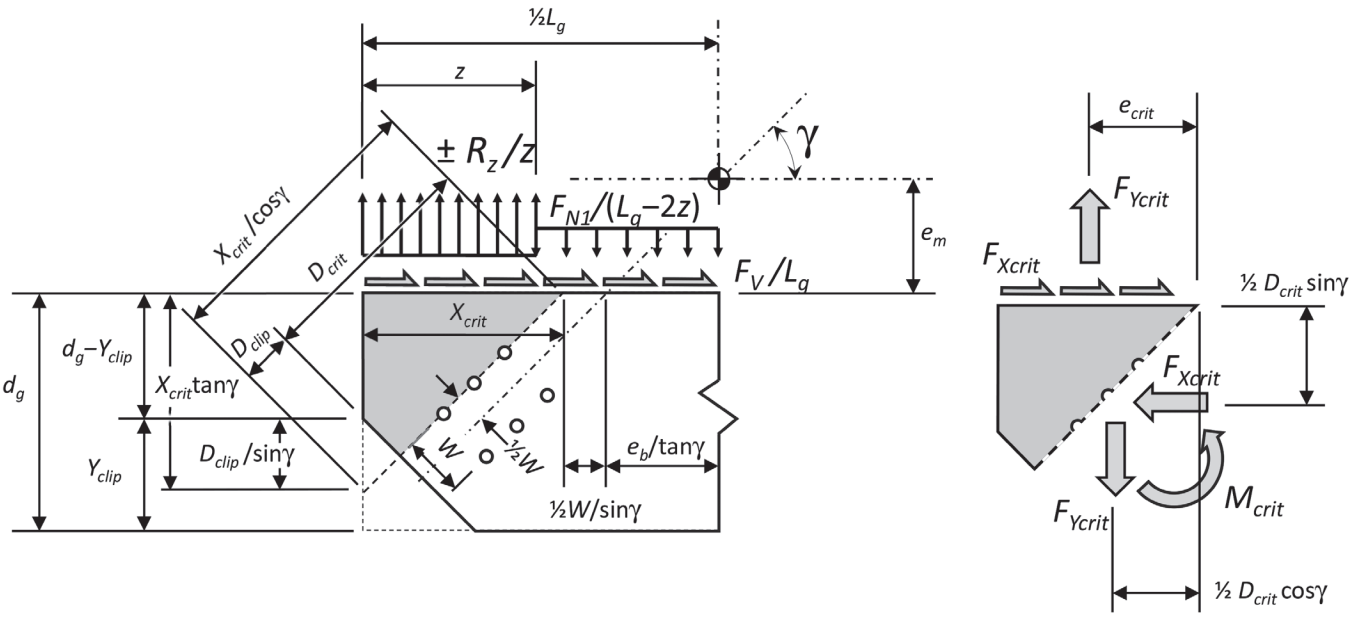

Fig. 19. Critical gusset section.

$$M_{crit} = F_{Ycrit}\left(e_{crit} - \frac{D_{crit}\cos\gamma}{2}\right) + F_{Xcrit}\frac{D_{crit}\sin\gamma}{2} \quad (83)$$

The forces are transformed to act on the diagonal section:

$$V_{crit} = F_{Xcrit}\cos\gamma + F_{Ycrit}\sin\gamma \quad (84)$$

$$N_{crit} = F_{Xcrit}\sin\gamma - F_{Ycrit}\cos\gamma \quad (85)$$

The gusset should be evaluated for these forces using an interaction method such as the von Mises yield criterion or interaction Equation 9-1 in the AISC *Steel Construction Manual*.

Weld Design

The design of welds should provide adequate strength to transfer forces across the gusset-to-beam interface (F_V, F_N, and M_f) and adequate ductility to achieve the assumed stress distribution. The weld size for a double fillet need not exceed ⅝ of the gusset thickness (for an adequately sized gusset), as discussed for single-plate connections in the AISC *Steel Construction Manual* (2017); this weld size permits yielding of the gusset before weld rupture. (This proportioning rule implicitly accepts use of a resistance factor greater than 0.75.) Weld sizes greater than ⅝ of the gusset thickness are not effective in developing their full force because they are limited by the gusset capacity (and thus also indicate an inadequate gusset thickness); however, increasing a weld that requires less than ⅝ of the gusset thickness up to this value allows for yielding of the gusset before weld rupture and thus permits stress redistribution.

Uniform Stress Method

Under the Uniform Stress Method, the weld adequacy should be evaluated using methods from the AISC *Steel Construction Manual*, such as the instantaneous center of rotation, which represents both weld strength and the limits on weld ductility. As a minimum, the weld should be large enough to resist the local stress consistent with the Uniform Stress Method. The required strength per unit length is:

$$r_u = \sqrt{\left(\frac{|4M_{f1}|}{L_{g1}^2} + \frac{|F_{N1}|}{L_{g1}}\right)^2 + \left(\frac{F_{V1}}{L_{g1}}\right)^2} \quad (86)$$

The AISC *Seismic Design Manual* (2018) utilizes the 25% increase related to gussets at beam-column-brace connections to promote ductility per the AISC *Steel Construction Manual* and Hewitt and Thornton (2004). Hadad and Fortney (2020) determined a ratio of maximum to average stress of approximately 3 (including a standard deviation) for weld stresses in their finite element analyses of chevron connections. They suggest that the factor of 3 be applied in the design of the weld (which need not exceed the size corresponding to the gusset-plate strength).

Concentrated Stress Method

The Concentrated Stress Method inherently addresses nonuniform stress in the gusset and may indicate stresses in the z region much higher than indicated by the Uniform Stress Method. As such, the increase to address nonuniform stress is not proposed for this method.

For designs employing the Concentrated Stress Method, stresses may redistribute along the weld due to beam inelasticity. As such, the stress distribution corresponding to the instantaneous center of rotation method may be impossible to achieve with the beam web strength provided. The weld in the z_1 zones should be evaluated for the force normal to the member axis, R_{z1}. For welds in the center region ($L_{g1} - 2z_1$), the normal force is F_{N1}. The shear force (parallel to the member axis) in both regions may be taken as F_{V1}/L_{g1}. Often the weld size required in the z regions will be substantially greater than that required in the center region.

To address strain compatibility of the linear weld group consisting of a larger weld size in the z regions and a smaller size in the center, two measures are proposed. First, the weld size in the z region may be sized to develop the strength of the gusset plate (e.g., a double fillet weld of at least ⅝ of the gusset thickness); this ensures that the deformation required of that zone of the joint may be provided by the gusset, and thus the full strength of both that region and the center region can be achieved.

Second, the two welds may be proportioned so that their strains are consistent with the design strength utilized. This may be done by analyzing the deformation of the different weld elements, as in the instantaneous center of rotation method. The authors have found satisfactory designs by proportioning the weld group with the weld in the center zone being ⅝ of the size of the welds in the z region and then extending the larger z-region weld to the ¼ point of the gusset at each end. It is expected that, with more study, those minima could be reduced or eliminated. Alternatively, the weld size selected for the z region may be used for the entire gusset length.

PROPOSED DESIGN PROCEDURE

The design of chevron and full-height gussets may be governed by design considerations other than the local forces addressed in this paper. In such cases, the material efficiency of the Concentrated Stress Method cannot be realized, and the Uniform Stress Method (which is simpler to implement) may be convenient. The following design procedure may be used to minimize the complexity of the required calculations:

1. Establish parameters.

   1.1 Determine the forces F_V, F_N, and M_f, acting on the gusset-member interface.

   1.2 Determine the optimal gusset-plate length based on the brace-to-gusset connection (and any other considerations). If desired, determine the optimal gusset thickness.

   1.3 For connections with gussets on opposite flanges, determine shear-strength apportionment for the two gussets per Equations 51 and 52.

2. Try the Uniform Stress Method.

   2.1. Check if the optimal gusset-plate length exceeds the minimum length required for the Uniform Stress Method using Equation 15 or 55. If so:

   2.2. Check member.

      2.2.1. Determine V_{mc} (Equation 14); check shear.

      2.2.2. Evaluate web local yielding and web crippling Equation 17.

   2.3. Design gusset.

      2.3.1. Design the gusset section parallel to the member axis using the Uniform Stress Method Equation 63.

      2.3.2. Check the transverse gusset section for the forces from Equations 65, 66, and 68. (Any procedure in the AISC *Manual* may be used.)

   2.4. Design the gusset–member interface weld. (Design for peak stress using the Uniform Stress Method distribution; apply appropriate ductility factor or size to develop the gusset plate strength.)

3. If the Uniform Stress Method design is unsatisfactory, try the Concentrated Stress Method.

   3.1 Select gusset length.

      3.1.1. Check minimum length required for the Concentrated Stress Method (Equation 34). Use the maximum of the optimal gusset-plate length and this minimum length. If this length is excessive, consider reinforcing the member web (or using a different member).

      3.1.2. Determine the required gusset thickness per Equations 36 and 38. Revise gusset length if necessary.

   3.2. Analyze connection and check member

      3.2.1. Determine the length of the zone z (Equations 40, 41, and 42). Use the maximum length from these three equations.

      3.2.2. Determine the concentrated force R_z (Equation 26).

      3.2.3. Determine V_{mc} (Equation 27); check member shear.

   3.3. Design gusset.

      3.3.1. Check the gusset section at the interface with the flange in the center zone. (Gusset horizontal section at the interface with the flange in the z zone is implicitly checked by the required thickness calculation.)

      3.3.2. Check the transverse gusset section for the forces from Equations 65, 69, and 71. (Any procedure in the AISC *Manual* may be used.)

      3.3.3. Check the diagonal gusset section for the forces from Equations 80 (or 83), 84, and 85. (Any procedure in the AISC *Manual* may be used.)

   3.4 Design weld.

      3.4.1. Design zone z weld.

      3.4.2. Design center-zone weld.

Note that this recommended design procedure implicitly checks member shear in the connection region for both the Uniform Stress Method and the Concentrated Stress Method. It does not include a check of the member for combined axial and bending forces within the connection region based on the authors' experience and judgment.

Table 1. Brace Forces			
	Brace Axial Force *F* (kips)	**Shear Component *F* cos(γ) (kips)**	**Normal Component *F* sin(γ) (kips)**
$F_{1,1}$	568	364	436
$F_{1,2}$	653	418	502
$F_{2,2}$	511	327	393
$F_{2,1}$	588	376	451

DESIGN EXAMPLE

The connection shown in Figure 20 will be designed following the recommended procedure, proceeding from the Uniform Stress Method to the Concentrated Stress Method developed in this study to eliminate reinforcement.

Given:

The brace design forces are presented in Table 1. All brace angles are 50.2° from horizontal. To facilitate subsequent calculations, the shear and normal components of the brace forces are determined and presented in the table.

Both beam and gusset are Grade 50 material. The beam is a W24×94 (ϕV_n = 375 kips; A=27.7 in.^{2}; Z=254 in.^{4}), 25 feet long. The workpoint is at the beam centerline:

$$e_m = \frac{d_m}{2} = 12.15 \text{ in.} \tag{8}$$

The beam moment due to loading other than from braces, M_M, is 80 kip-ft.

Based on the brace-to-gusset connection (not shown), the minimum gusset length is 48 in. For the brace-to-gusset connection design, a ¾-in.-thick gusset is optimal, and the depth required is 21 in.

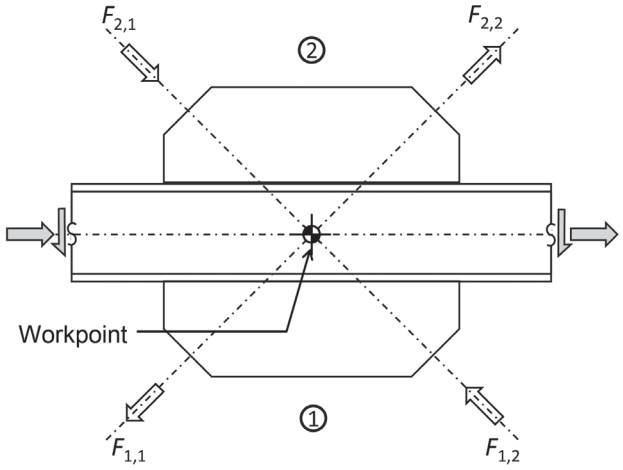

Fig. 20. Design example.

Table 2. Connection Forces				
	Equation	Gusset 1	Gusset 2	Combination (total or difference)
$F_{V\,(i)}$ (kips)	1	782	703	78.5
$F_{N\,(i)}$ (kips)	2	65.5	58.9	6.6
$M_{f\,(i)}$ (kip-in.)	3	9500	8550	18000
$V_{ef\,(i)}/V_{efTOT}$	51; 52	0.526	0.474	1.0

Solution:

Design of Gusset 1

1. Establish Parameters

Optimal gusset dimensions have been given. The forces acting on the flange from each of the gussets is shown in Table 2, which also shows the apportionment factors for beam effective shear strength.

2. Try the Uniform Stress Method

The minimum gusset length is determined from:

$$\begin{aligned} L_g &\geq \frac{2M_{Tot}}{V_{efTot}} \\ &= \frac{18{,}000 \text{ kip-in.}}{375 \text{ kips}} \\ &= 96.1 \text{ in.} \end{aligned} \tag{55}$$

For 48-in. gussets both above and below the beam, the Uniform Stress Method requires a web thickness of:

$$\begin{aligned} t_w &\geq \frac{F_{V1}/L_{g1} + F_{V2}/L_{g2}}{\phi_v 0.6F_y} \\ &= \frac{F_{V1} + F_{V2}}{\phi_v 0.6F_y L_g} \\ &= \frac{782 \text{ kips} + 703 \text{ kips}}{(1.0)0.6(50 \text{ ksi})(48 \text{ in.})} \\ &= 1.03 \text{ in.} \end{aligned} \tag{62}$$

This would require a W24×250. (Using the same gusset length, a W21×248 or a W18×211 would also be suitable.) Alternatively, an increase in effective shear strength of 96.1/48 = 2.0 could be achieved by a web doubler of ¾ × 18 in.:

$$\begin{aligned} L_g &\geq \frac{2M_{Tot}}{V_{efTot}} \\ &= \frac{2M_{Tot}}{(\phi_v V_{n_{beam}} + \phi_v V_{n_{doubler}})} \\ &= \frac{2(18{,}000 \text{ kip-in.})}{[375 \text{ kips} + 1.0(0.6)(0.75 \text{ in.})(18 \text{ in.})(50 \text{ ksi})]} \\ &= 46.2 \text{ in.} \end{aligned} \tag{55}$$

The minimum extents of the doubler can be determined using Equation 13.

The Uniform Stress Method would require a 96-in. gusset without reinforcement, a much heavier beam, or significant reinforcement to permit a gusset on the order of the optimal 48-in. length. As none of these is desirable, the design will proceed with the Concentrated Stress Method.

3. Try the Concentrated Stress Method

For the Concentrated Stress Method, the effective shear strength, V_{efTOT}, must be reduced considering the net unbalanced force:

$$V_{efTot} = \phi_v V_n - \left| \frac{F_{N1}}{2} - \frac{F_{N2}}{2} \right| \tag{56}$$
$$= 375 \text{ kips} - \left| \frac{6.6 \text{ kips}}{2} \right|$$
$$= 372 \text{ kips}$$

The lower gusset will be designed to utilize no more than 52.6% of the available member shear strength per Equation 51.

$$V_{ef1} = \frac{M_{f1}}{M_{Tot}} V_{efTot} \tag{51}$$
$$= \frac{9{,}500 \text{ kip-in.}}{18{,}000 \text{ kip-in.}} (372 \text{ kips})$$
$$= 196 \text{ kips}$$

Minimum Gusset Length and Corresponding Thickness

Assuming (for preliminary design) that the transverse force R_{z1} is equal to this effective shear strength, the minimum gusset length is:

$$L_{g1} > \frac{M_{f1}}{V_{ef1}} + \frac{V_{ef1}}{\phi_w F_y t_w} - 5k \tag{34}$$
$$= \frac{9{,}500 \text{ kip-in.}}{196 \text{ kips}} + \frac{196 \text{ kips}}{(1.0)(50 \text{ ksi})(0.515 \text{ in.})} - 5(1.38 \text{ in.})$$
$$= 49.2 \text{ in.}$$

The approximate length that corresponds to a ¾-in. gusset is:

$$L_{g1} > \frac{M_{f1}}{V_{ef1}} + \frac{V_{ef1}}{\phi_t F_y t_{g1}} \tag{39}$$
$$= \frac{9{,}500 \text{ kip-in.}}{196 \text{ kips}} + \frac{196 \text{ kips}}{(0.9)(50 \text{ ksi})(0.75 \text{ in.})}$$
$$= 54.3 \text{ in.}$$

As this length does not include the effect of the shear, a slightly larger value will be used, and the effect of shear addressed in the determination of the minimum length z_1. A 56-in. effective gusset length will be investigated. (The length also results in an economical weld design, which is presented later in the example.) The detailed length is 58 in., recognizing that the weld will not extend to the very end of the gusset.

The minimum bearing length z_1 based on the limit states of web local yielding and web crippling is:

$$z_1 \geq \frac{L_{g1}}{2} - \sqrt{\frac{L_{g1}^2}{4} - \frac{M_{f1}}{\phi_w F_y t_w}} - 5k \tag{40}$$

$$= \frac{56.0 \text{ in.}}{2} - \sqrt{\frac{(56.0 \text{ in.})^2}{4} - \frac{9{,}500 \text{ kip-in.}}{(1.0)(50 \text{ ksi})(0.515 \text{ in.})}} - 5(1.38 \text{ in.})$$

$$= 0.73 \text{ in.}$$

$$z_1 \geq \left[\frac{V_{ef1}}{\phi_n 0.80 t_w^2}\sqrt{\frac{t_w}{EF_y t_f}} - 1\right]\left(\frac{d_m}{3}\right)\left(\frac{t_f}{t_w}\right)^{1.5} \tag{42}$$

$$= \left[\frac{196 \text{ kips}}{(0.75)(0.80)(0.515 \text{ in.})^2}\sqrt{\frac{0.515 \text{ in.}}{(29{,}000 \text{ ksi})(50 \text{ ksi})(0.875 \text{ in.})}} - 1\right]\left(\frac{24.3 \text{ in.}}{3}\right)\left(\frac{0.875 \text{ in.}}{0.515 \text{ in.}}\right)^{1.5}$$

$$= -3.87 \text{ in.}$$

The low value from Equation 40 and the negative value from Equation 42 indicate that the force being developed, R_z, does not require a significant bearing length to satisfy the limit states of web local yielding and web crippling.

The minimum length z_1 corresponding von Mises yield criterion for stresses in the gusset is obtained from Equation 41:

$$z_1 = \frac{L_{g1}}{2} - \sqrt{\frac{{L_{g1}}^2}{4} - \frac{M_{f1}/\phi_t}{\sqrt{(F_y t_{g1})^2 - \left(\frac{F_{V1}}{\phi_v 0.6 L_{g1}}\right)^2}}} \tag{41}$$

$$= \frac{56.0 \text{ in.}}{2} - \sqrt{\frac{(56.0 \text{ in.})^2}{4} - \frac{9{,}500 \text{ kip-in.}/0.9}{\sqrt{[(50 \text{ ksi})(0.75 \text{ in.})]^2 - \left(\frac{782 \text{ kips}}{(1.0)(0.6)(56 \text{ in.})}\right)^2}}}$$

$$= 7.38 \text{ in.}$$

The maximum length z_1 is:

$$z_1 \leq L_{g1} - \frac{M_{f1}}{V_{ef_1}} \tag{43}$$

$$= 56.0 \text{ in.} - \frac{9{,}500 \text{ kip-in.}}{196 \text{ kips}}$$

$$= 7.51 \text{ in.}$$

The value from Equation 41 will be used. The corresponding transverse force is:

$$R_{z1} = \frac{M_{f1}}{L_{g1} - z_1} \tag{26}$$

$$= \frac{9{,}500 \text{ kip-in.}}{56.0 \text{ in.} - 7.38 \text{ in.}}$$

$$= 195 \text{ kips}$$

The limit states of web local yielding, web crippling, and gusset combined tension and shear yielding are implicitly checked by the gusset-length selection and this length z_1 determined above (Equations 40, 42, and 41). This value may also be used to check gusset stress using Equation 36; however, gusset stress is implicitly checked by the selection of a dimension z_1 that complies with Equation 41.

The beam shear is evaluated considering 52.6% of the shear due to the total unbalanced force:

$$V_{mc1} = V_{ma1} + R_{z1} \tag{27}$$

$$= \left(\frac{M_{f1}}{M_{Tot}}\right)\frac{F_{N1} - F_{N2}}{2} + R_{z1}$$

$$= 0.526\left(\frac{6.6 \text{ kips}}{2}\right) + (195 \text{ kips})$$

$$= 197 \text{ kips}$$

$$\frac{V_{mc1}}{\phi_v V_n} = \frac{197 \text{ kips}}{375 \text{ kips}}$$

$$= 0.525 \le 0.526 \quad \textbf{o.k.}$$

This is consistent with the apportionment of available beam shear strength between the two gussets established in Table 2.

Beam Moment and Axial Force in Gusset Region

For completeness, the combined effects of the internal beam moment and axial force are evaluated. (The proposed design procedure does not include this evaluation.)

Although Equation 49 permits a more precise calculation of beam moment, the moment is typically small, and the upper-bound value is used here for convenience for gusset 2, as that design has not been performed. Adapting Equation 49 to include the effect of two gussets gives:

$$M_{max} = \frac{M_{Ch1}}{2}\left[\frac{z_1}{L_{g1}} - \left(\frac{z_1}{L_{g1}}\right)^2\right] + \frac{M_{Ch2}}{2}\left[\frac{z_2}{L_{g2}} - \left(\frac{z_2}{L_{g2}}\right)^2\right] + \frac{(F_{N1} - F_{N2})L_{beam}}{4} + M_M$$

For gusset 1:

$$\frac{1}{2}\left[\frac{z_1}{L_{g1}} - \left(\frac{z_1}{L_{g1}}\right)^2\right] = \frac{1}{2}\left[\frac{7.38 \text{ in.}}{56.0 \text{ in.}} - \left(\frac{7.38 \text{ in.}}{56.0 \text{ in.}}\right)^2\right]$$

$$= 0.0572$$

For gusset 2, the dimension z_2 has not been determined. In this example (with $M_{f2} < M_{f1}$), z_2 could reasonably be assumed to be less than or equal to z_1 if $L_{g2} = L_{g1}$. The general limit is:

$$\frac{1}{2}\left[\frac{z_2}{L_{g2}} - \left(\frac{z_2}{L_{g2}}\right)^2\right] \le \frac{1}{8}$$

$$M_{max} \le 0.0572\left(\frac{9{,}500 \text{ kip-in.}}{12 \text{ in./ft}}\right) + 0.125\left(\frac{8{,}550 \text{ kip-in.}}{12 \text{ in./ft}}\right) + \frac{(65.5 \text{ kips} - 58.9 \text{ kips})(25 \text{ ft})}{4} + 80 \text{ kip-ft}$$

$$\le 255 \text{ kip-ft}$$

The axial force is conservatively taken as the maximum at the end of the connection region, assuming a symmetric distribution of collector forces:

$$P_u = \left|\frac{F_{V1}}{2} - \frac{F_{V2}}{2}\right|$$

$$= \left|\frac{782 \text{ kips}}{2} - \frac{703 \text{ kips}}{2}\right|$$

$$= 39.5 \text{ kips}$$

Assuming the section is fully braced at this location, the full section strength is used:

$$\phi_c P_n = \phi_c A_s F_y$$
$$= (0.9)(27.7 \text{ in.}^2)(50 \text{ ksi})$$
$$= 1{,}250 \text{ kips}$$

$$\phi_b M_n = \phi_b Z F_y$$
$$= (0.9)(254 \text{ in.}^3)(50 \text{ ksi})$$
$$= 11{,}400 \text{ kip-in.}$$
$$= 953 \text{ kip-ft.}$$

$$\frac{P_u}{\phi_c P_n} = 0.03$$

$$\frac{M_u}{\phi_b M_n} = 0.27$$

The interaction check from AISC *Specification* Equation H1-1b is used:

$$\frac{1}{2}\frac{P_u}{\phi_c P_n} + \frac{M_u}{\phi_b M_n} = \frac{1}{2}(0.06) + 0.27 \qquad \text{(from } \textit{Spec.} \text{ Eq. H1-1b)}$$
$$= 0.30 \quad \textbf{o.k.}$$

Gusset Selection

A ¾-in.-thick, 21-in.-deep, and 58-in.-long (56-in. effective length) gusset will be investigated.

$t_{g1} = 0.75$ in.
$d_{g1} = 21.0$ in.
$L_{g1} = 56.0$ in.

Gusset Check at Section Parallel to the Member Axis at Beam Flange

The Concentrated Stress Method implicitly checks the gusset over the lengths z_1 for combined stresses in determining the minimum length z_1 (Equation 41). For the center zone between the lengths z_1, Equation 38 gives the interaction ratio:

$$\sqrt{\left(\frac{F_{V1}}{\phi_v 0.6 F_y t_{g1} L_{g1}}\right)^2 + \left(\frac{F_{N1}}{\phi_t F_y t_{g1}(L_{g1} - 2z_1)}\right)^2} \qquad (38)$$
$$= \sqrt{\left[\frac{782 \text{ kips}}{0.6(50 \text{ ksi})(0.75 \text{ in.})(56.0 \text{ in.})}\right]^2 + \left\{\frac{65.5 \text{ kips}}{(0.9)(50 \text{ ksi})(0.75 \text{ in.})[56.0 \text{ in.} - 2(7.38 \text{ in.})]}\right\}^2}$$
$$= 0.622$$

Gusset Check at Mid-Length Transverse Section

The adequacy of the gusset depth is verified examining a section of the gusset transverse to the member axis. (See Figure 18.) The gusset force in direction of member is:

$$N_{g1} = \frac{1}{2}(F_{1,2}\cos\gamma_{1,2} - F_{1,1}\cos\gamma_{1,1}) \qquad (65)$$
$$= \frac{1}{2}(418 \text{ kips} - 364 \text{ kips})$$
$$= 27 \text{ kips}$$

The axial resistance of the gusset is:

$$\begin{aligned}\phi_t P_n &= 0.9 F_y d_{g1} t_{g1} \\ &= (0.9)(50 \text{ ksi})(21.0 \text{ in.})(0.75 \text{ in.}) \\ &= 709 \text{ kips}\end{aligned}$$

The gusset moment is:

$$\begin{aligned}M_{g1} &= N_{g1}\left(e_m + \frac{d_{g1}}{2}\right) - \frac{F_{N1}}{2}\left(\frac{L_{g1}}{4} - \frac{z_1}{2}\right) \\ &= (27 \text{ kips})\left(12.15 \text{ in.} + \frac{21.0 \text{ in.}}{2}\right) - \frac{65.5 \text{ kips}}{2}\left(\frac{56 \text{ in.}}{4} - \frac{7.38 \text{ in.}}{2}\right) \\ &= 280 \text{ kip-in.}\end{aligned} \tag{71}$$

The flexural resistance of the gusset is:

$$\begin{aligned}\phi_b M_n &= 0.9 F_y \frac{d_{g1}^2 t_{g1}}{4} \\ &= 0.9(50 \text{ ksi})\frac{(21.0 \text{ in.})^2 (0.75 \text{ in.})}{4} \\ &= 3{,}720 \text{ kip-in.}\end{aligned}$$

Gusset shear transverse to member:

$$\begin{aligned}V_{g1} &= F_{1,1} \sin\gamma_{1,1} - R_{z1} + \frac{F_{N1}}{2} \\ &= 436 \text{ kips} - 195 \text{ kips} + \frac{65.5 \text{ kips}}{2} \\ &= 274 \text{ kips}\end{aligned} \tag{69}$$

The shear resistance is:

$$\begin{aligned}\phi_v V_n &= 1.00(0.60 F_y) d_{g1} t_{g1} \\ &= 1.00(0.60)(50 \text{ ksi})(21.0 \text{ in.})(0.75 \text{ in.}) \\ &= 473 \text{ kips}\end{aligned}$$

Using the von Mises interaction equation:

$$\begin{aligned}\sqrt{\left(\frac{M_{g1}}{\phi_t M_n} + \frac{N_{g1}}{\phi_t P_n}\right)^2 + \left(\frac{V_{g1}}{\phi_v V_n}\right)^2} &= \sqrt{\left(\frac{280 \text{ kip-in.}}{3{,}720 \text{ kip-in.}} + \frac{27 \text{ kips}}{709 \text{ kips}}\right)^2 + \left(\frac{274 \text{ kips}}{473 \text{ kips}}\right)^2} \\ &= 0.590\end{aligned}$$

Gusset Check along Diagonal Section

The gusset will be checked along the critical diagonal section (Figure 19). The bolt gage, W, is 8 in. and the transverse dimension Y_{clip} is 8.0 in.

$$\begin{aligned}X_{crit} &= \frac{L_{g1}}{2} - \frac{d_m \cos\gamma + W}{2\sin\gamma} \\ &= \frac{56.0 \text{ in.}}{2} - \frac{(24.3 \text{ in.})\cos(50.2°) + 8 \text{ in.}}{2\sin(50.2°)} \\ &= 12.7 \text{ in.}\end{aligned} \tag{72}$$

This value is greater than z_1.

The diagonal section length is:

$$D_{crit} = X_{crit}\cos\gamma + (d_{g1} - Y_{clip})\sin\gamma \tag{75}$$
$$= (12.7\text{ in.})\cos(50.2°) + (21.0\text{ in.} - 8\text{ in.})\sin(50.2°)$$
$$= 18.1\text{ in.}$$

The forces acting on the section are:

$$F_{Xcrit} = \frac{X_{crit}}{L_{g1}} F_{V1} \tag{77}$$
$$= \frac{12.7\text{ in.}}{56.0\text{ in.}}(782\text{ kips})$$
$$= 177\text{ kips}$$

$$F_{Ycrit} = R_{z1} + F_{N1}\frac{X_{crit} - z_1}{L_{g1} - 2z_1} \tag{81}$$
$$= 195\text{ kips} + (65.5\text{ kips})\frac{12.7\text{ in.} - 7.38\text{ in.}}{56.0\text{ in.} - 2(7.38\text{ in.})}$$
$$= 204\text{ kips}$$

$$e_{crit} = \frac{R_{z1}\left(X_{crit} - \frac{z_1}{2}\right) + F_{N1}\frac{(X_{crit} - z_1)^2}{2(L_g - 2z_1)}}{F_{Ycrit}} \tag{82}$$
$$= \frac{(195\text{ kips})\left(195\text{ kips} - \frac{7.38\text{ in.}}{2}\right) + (65.5\text{ kips})\frac{(12.7\text{ in.} - 7.38\text{ in.})^2}{2[56.0\text{ in.} - 2(7.38\text{ in.})]}}{204\text{ kips}}$$
$$= 8.72\text{ in.}$$

$$M_{crit} = F_{Ycrit}\left(e_{crit} - \frac{D_{crit}\cos\gamma}{2}\right) + F_{Xcrit}\frac{D_{crit}\sin\gamma}{2} \tag{83}$$
$$= (204\text{ kips})\left[8.72\text{ in.} - \frac{(18.1\text{ in.})\cos(50.2°)}{2}\right] + (177\text{ kips})\frac{(18.1\text{ in.})\sin(50.2°)}{2}$$
$$= 1{,}825\text{ kip-in.}$$

$$V_{crit} = F_{Xcrit}\cos\gamma + F_{Ycrit}\sin\gamma \tag{84}$$
$$= 270\text{ kips}$$

$$N_{crit} = F_{Xcrit}\sin\gamma - F_{Ycrit}\cos\gamma \tag{85}$$
$$= (177\text{ kips})\sin(50.2°) - (204\text{ kips})\cos(50.2°)$$
$$= 5\text{ kips}$$

The gusset is evaluated for these forces using the von Mises yield criterion:

$$\sqrt{\left(\frac{4|M_{crit}|}{\phi_t F_y t_{g1} {D_{crit}}^2} + \frac{N_{crit}}{\phi_t F_y t_{g1} D_{crit}}\right)^2 + \left(\frac{V_{crit}}{\phi_v 0.6 F_y t_{g1} D_{crit}}\right)^2}$$
$$= \sqrt{\left[\frac{4(1{,}825\text{ kip-in.})}{(0.9)(50\text{ ksi})(0.75\text{ in.})(18.1\text{ in.})^2} + \frac{5\text{ kips}}{(0.9)(50\text{ ksi})(0.75\text{ in.})(18.1\text{ in.})}\right]^2 + \left[\frac{270\text{ kips}}{1.00(0.60)(50\text{ ksi})(0.75\text{ in.})(18.1\text{ in.})}\right]^2}$$
$$= 0.94 \le 1.0 \quad \textbf{o.k.}$$

Gusset Weld (z-Region)

The weld along the length z_1 must deliver a normal force equal to R_{z1}; it must also deliver a shear force proportional to its length:

$$N_{weld} = R_{z1}$$
$$= 195 \text{ kips}$$

$$V_{weld} = \frac{z_1}{L_g} F_{v1}$$
$$= \frac{7.38 \text{ in.}}{56.0 \text{ in.}}(782 \text{ kips})$$
$$= 103 \text{ kips}$$

The weld in this zone therefore resists a force at an angle:

$$P_u = \sqrt{N_{weld}{}^2 + V_{weld}{}^2}$$
$$= \sqrt{(195 \text{ kips})^2 + (103 \text{ kips})^2}$$
$$= 221 \text{ kips}$$

The angle θ is $\tan^{-1}(195/103) = 62°$ from the weld axis. Using AISC *Specification* Equation J2-5:

$$P_u \le \phi R_n$$
$$= \phi_n 0.6 F_{EXX} (1.0 + 0.5 \sin^{1.5} \theta) \frac{\sqrt{2}}{2} w L_w$$
$$w \ge \frac{P_u}{\phi_n 0.6 F_{EXX} (1.0 + 0.5 \sin^{1.5} \theta) \frac{\sqrt{2}}{2} (2 z_1)}$$
$$w \ge \frac{221 \text{ kips}}{(0.75) 0.6 (70 \text{ ksi}) \left[1.0 + 0.5 \sin^{1.5} (62.2°)\right] \sqrt{2} (7.38 \text{ in.})}$$
$$= 0.474 \text{ in.}$$

A double-sided ½-in. fillet weld will be used. The weld size need not exceed ⅝ of the gusset plate thickness:

$$w \le \frac{5}{8} t_{g1}$$
$$= \frac{5}{8}(0.75 \text{ in.})$$
$$= 0.469 \text{ in.}$$

This weld must include the z region; a 14-in. length will be used to extend to the gusset ¼ points. Because this weld fully develops the gusset strength, deformation compatibility is inherently addressed.

Gusset Weld (Center Region)

The weld in the center region must be checked. The required strength is based on:

$$L_{g1} - 2z_1 = 56.0 \text{ in.} - 2(7.38 \text{ in.})$$
$$= 41.2 \text{ in.}$$

$$N_{weld} = F_{N1}$$
$$= 65.5 \text{ kips}$$

$$V_{weld} = F_{V1}\frac{L_{g1} - 2z_1}{L_{g1}}$$
$$= (782 \text{ kips})\frac{56.0 \text{ in.} - 2(7.38 \text{ in.})}{56.0 \text{ in.}}$$
$$= 576 \text{ kips}$$
$$P_u = \sqrt{N_{weld}{}^2 + V_{weld}{}^2}$$
$$= \sqrt{(65.5 \text{ kips})^2 + (576 \text{ kips})^2}$$
$$= 579 \text{ kips}$$

The angle θ is $\tan^{-1}(65.5/576) = 6.5°$. Using AISC *Specification* Equation J2-5:

$$w \geq \frac{P_u}{\phi_n 0.6F_{EXX}(1.0 + 0.5\sin^{1.5}\theta)\frac{\sqrt{2}}{2}2(L_{g1} - 2z_1)}$$
$$= \frac{579 \text{ kips}}{(0.75)0.6(70 \text{ ksi})\left[1.0 + 0.5\sin^{1.5}(6.5°)\right]\sqrt{2}(41.2 \text{ in.})}$$
$$= 0.310 \text{ in.}$$

A pair of the 5⁄16-in. fillet welds will be used.

The weld group consisting of the *z*-region and center welds conforms to both of the deformation compatibility recommendations: the *z*-region welds develop the gusset strength and extend to the gusset ¼ points, and the center region welds are ⅝ of the size of the welds in the *z*-regions.

Design Summary

Figure 21 shows the design based on the calculations above. The ½-in. fillet welds in the *z*-regions are presented as 3⁄16-in. fillet welds over the 5⁄16-in. full-length fillet welds.

A similar design is required for gusset 2. If the same method is followed, the beam shear resulting from the two gussets (each designed for a portion of V_{ef}) combined with the net unbalanced load will not exceed the beam shear capacity.

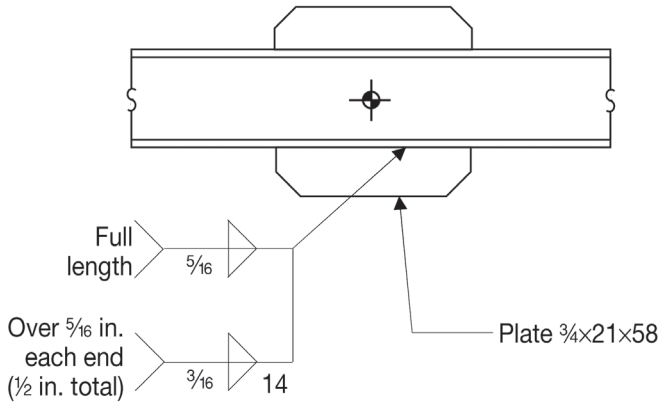

Fig. 21. Gusset design.

CONCLUSIONS

This study provides equations that can be used in the design of bracing connections to eliminate the need for web reinforcement. Recommendations are made for the selection of braced-frame beams and columns to facilitate connection design. The design method allows engineers to use the gusset plate to limit the shear demand on the member web. These equations can be used to assess the effects of member depth and gusset length on the required member shear strength in order to optimize member selection and gusset design. The Concentrated Stress Method presented allows for significantly smaller gusset plates than the Uniform Stress Method for an unreinforced section. For cases in which the Uniform Stress Method requires an undesirably large gusset or the use of a web doubler, the Concentrated Stress Method may permit a more economical design.

ACKNOWLEDGMENTS

The authors would like to recognize their debt to the pioneering work of William Thornton and the late Pat Fortney. Leigh Arber provided invaluable assistance in the review of this paper.

REFERENCES

AISC (2012), *Seismic Design Manual*, 2nd Ed., American Institute of Steel Construction, Chicago, Ill.

AISC (2016a), *Seismic Provisions for Structural Steel Buildings,* ANSI/AISC 341-16, American Institute of Steel Construction, Chicago, Ill.

AISC (2016b), *Specification for Structural Steel Buildings,* ANSI/AISC 360-16, American Institute of Steel Construction, Chicago, Ill.

AISC (2017), *Steel Construction Manual*, 15th Ed., American Institute of Steel Construction, Chicago, Ill.

AISC (2018), *Seismic Design Manual*, 3rd Ed., American Institute of Steel Construction, Chicago, Ill.

Euler, L. (translated by Hewlett, J.) [published 1765; 1822 translation], "Of a New Method of Resolving Equations of the Fourth Degree," *Elements of Algebra*, Longman, Hurst, Rees, Orme, and Company, London.

Fortney, P.J. and Thornton, W.A. (2015), "The Chevron Effect—Not an Isolated Problem," *Engineering Journal*, AISC, Vol. 52, No. 2, pp. 125–164.

Fortney, P.J. and Thornton, W.A. (2017), "The Chevron Effect and Analysis of Chevron Beams—A Paradigm Shift," *Engineering Journal*, AISC, Vol. 54, No. 4, pp. 263–296.

Hadad, A.A. and Fortney, P.J. (2020), "Investigation on the Performance of a Mathematical Model to Analyze Concentrically Braced Frame Beams with V-Type Bracing Configurations," *Engineering Journal*, AISC, Vol. 57, No. 2, pp. 91–108.

Hewitt, C.M. and Thornton, W.A. (2004), "Rationale Behind and Proper Application of the Ductility Factor for Bracing Connections Subjected to Shear and Transverse Loading," *Engineering Journal*, AISC, Vol. 41, No. 1, pp. 3–6.

Richards, P., Miller, B., and Linford, J. (2018), *Finite Element Evaluation of the Chevron Effect in Braced Frames,* Brigham Young University Report No. SSRP-2018/02.

Sabelli, R. and Arber, L. (2017), "Design of Chevron Gusset Plates," 2017 SEAOC Convention Proceedings.

Sabelli, R., Saxey, B., and Richards, P. (2020), "The Chevron Effect in Web Shear at Midspan Gussets," *Proceedings of the 17th World Conference on Earthquake Engineering*, Sendai, Japan.

Thornton, W.A. (1984), "Bracing Connections for Heavy Construction," *Engineering Journal*, AISC, Vol. 21, No. 3, pp. 139–148.

Discussion of: Design for Local Member Shear at Brace and Diagonal-Member Connections: Full-Height and Chevron Gusset

Original Paper by Rafael Sabelli and Brandt Saxey

Discussion by Paul W. Richards

ABSTRACT

The paper "Design for Local Member Shear at Brace and Diagonal-Member Connections: Full-Height and Chevron Gusset" (Sabelli and Saxey, 2021) develops equations for checking local member shear demands using a Concentrated Stress Method (CSM) and presents a design example. This discussion presents results from a finite element (FE) model, based on the design example in the paper, to quantify the accuracy of the proposed design equations in predicting beam yielding. The FE model confirmed that the beam yielding state would not have occurred for the example frame under the design forces but would have occurred for forces about 4% higher. The stress and strain distributions observed in the FE model were consistent with those assumed in the CSM, although two points for potential refinement were noted. If beam yielding in a concentrically braced frame is forced, through oversized braces, the plastic mechanism would be like an eccentrically braced frame (EBF) but with higher yield force and higher beam inelastic rotations and strains for the same inelastic story drift.

INTRODUCTION

The paper being discussed is one of several articles that have appeared in the AISC *Engineering Journal* addressing local member shear demands in braced frames (Fortney and Thornton, 2015, 2017; Fortney, 2020; Hadad and Thornton, 2022; Roeder et al., 2021; Sabelli and Bolin, 2022; Sabelli and Saxey, 2021; Sabelli et al., 2021). In the paper, the authors develop equations for checking local member shear demands in braced frames using a Concentrated Stress Method (CSM) and present a design example.

Figure 1 shows braced frames with different governing limit states. For seismic design, it is the intent of the *Seismic Provisions for Structural Steel Buildings* (AISC, 2016) that a brace yielding limit state govern [Figure 1(a)]. For nonseismic design, it could be fine for a beam shear yielding limit state to govern [Figure 1(b)], but the limit state needs to be checked explicitly to ensure that it is not reached under the design loads. Sabelli and Saxey (2021) outline the procedure for checking this beam shear yielding limit state [Figure 1(b)]. In their design example of a seismic frame, they use CSM to check beam yielding [Figure 1(b)] in order to ensure that brace yielding actually governs [Figure 1(a)].

Paul Richards, Vice President of Research and Development, DuraFuse Frames, West Jordan, Utah. Email: paul.richards@durafuseframes.com

Paper No. 2020-01D

In the paper, the authors cite previous work where finite element models were used to investigate beam shear demands in chevron frames (Richards et al., 2018). While results from those finite element (FE) models were consistent with the CSM design method, those FE models were somewhat limited in their ability to predict post-yield behavior.

The publication of Sabelli and Saxey (2021), including their thorough design example (CSM example), provided an opportunity for more robust FE validation. To determine the accuracy of their equations for checking beam shear yielding, FE analysis was performed on a model based on their design example. In the CSM example, the beam was capacity-designed based on the maximum forces that could be delivered by the braces [Figure 1(a)], but in the FE model, the braces were given unlimited strength to force the beam shear yielding mechanism [Figure 1(b)] to develop. The FE model answered three questions:

- Was the CSM used by Sabelli and Saxey (2021) accurate?
- What load would have caused shear yielding in the beam?
- What would have happened if a beam shear mechanism developed?

The answers to the first two questions are pertinent for new design. The answer to the last may be pertinent for some existing braced-frames where beam local shear yielding was not checked during design.

This discussion will describe the FE model and discuss the CSM example in the context of the FE model results.

FINITE ELEMENT MODEL

The geometry of the FE model matched that of the CSM example [Figure 2(a)]. The example frame connection had a W24×94 beam with gussets that had a 0.75 in. thickness and a 56 in. effective length (the gusset was 58 in. long, but the weld was held back 1 in. from each end). The four braces framing into the beam had an angle of 50.2° off horizontal. Figure 1(b) shows the maximum expected brace forces. The horizontal components in the lower story sum to 782 kips. The gusset was proportioned to be just long enough to preclude beam shear yielding under these forces (based on the CSM). The gusset-to-beam welds were ½ in. for the end segments (14 in. each end) and 5⁄16 in. for the 28 in. in the middle.

The FE model was developed and analyzed with ANSYS (2022). Three types of elements were used in the model to represent various components efficiently. The gusset plates, brace ends, welds, and beam (in the connection region) were

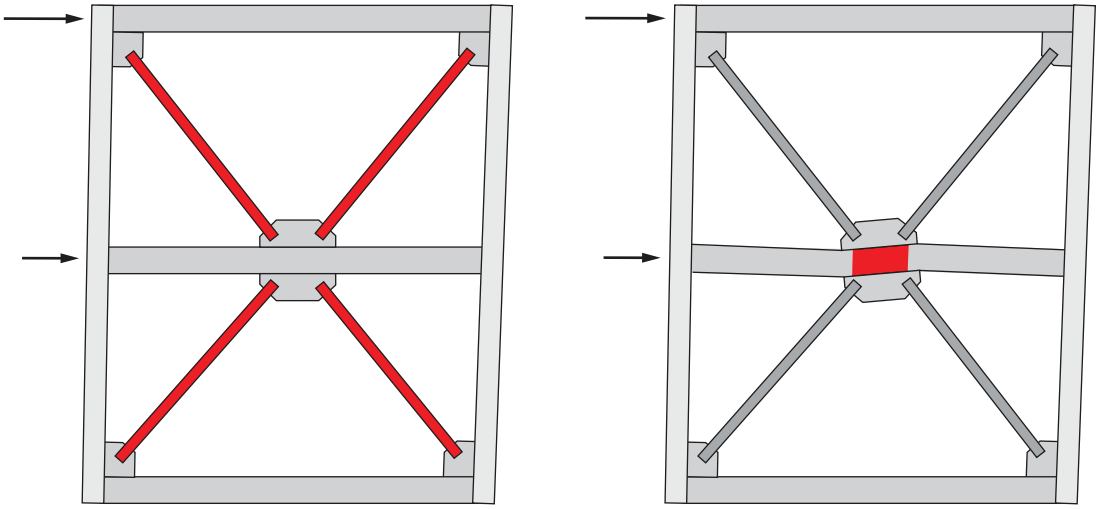

(a) Brace tension/compression yielding *(b) Beam shear yielding*

Fig. 1. Braced frames with different governing limit states.

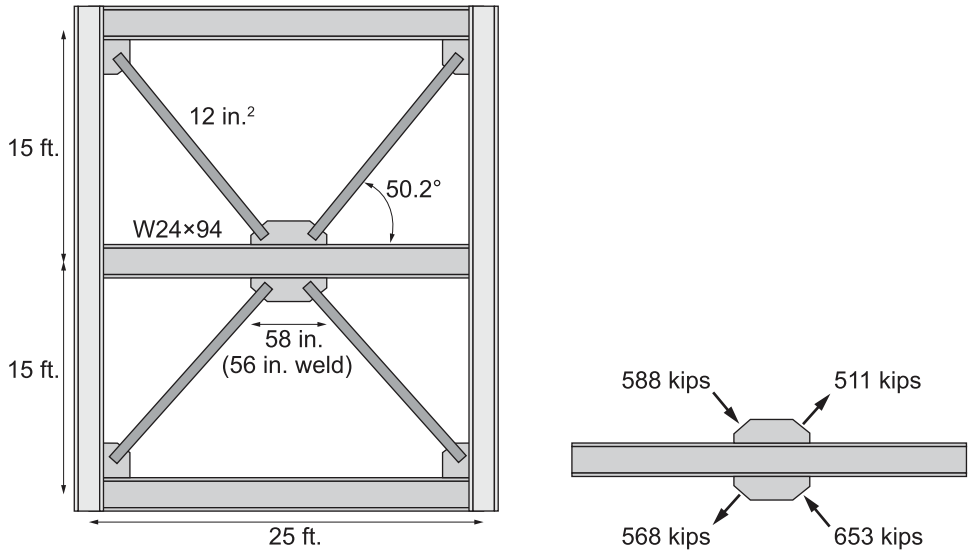

(a) Geometry *(b) Design loads*

Fig. 2. Frame from the CSM example.

modeled with solid elements (SOLID186) [Figure 3(a)-(c)]. The beam mesh in the connection region had an element dimension of 1 in. [Figure 3(b)]. The gusset-to-beam welds were modeled explicitly [Figure 3(c)]. Outside the gusset region, the beam was represented with elastic beam elements (BEAM188) [Figure 3(a)] with the cross-sectional properties of a W24×94. The braces were represented with elastic truss elements (LINK180) to force the beam shear yielding mechanism to form. Effective areas were used for the brace elements so that the magnitudes of the brace forces (relative to each other) would match the relative magnitudes of the forces in the design example [Figure 2(b)].

The boundary conditions and loading in the model were for a pushover-type analysis [Figure 3(a)]. The bottom nodes of the bottom braces were pinned in space. The beam ends and top brace nodes were on rollers that prevented movement in the *y*-direction and had displacements imposed in the *x*-direction. The relative magnitudes of the top and bottom applied displacements [0.526*x* in Figure 3(a)] were calibrated so that the magnitudes of the brace forces in the two stories would match the relative magnitudes of the forces in the design example [Figure 2(b)]. Out-of-plane restraint was applied to all nodes, including the beam web and gusset.

The materials in the FE model simulated nominal steel and weld properties. In the CSM example, the beam and gusset were Grade 50 material. In the FE model, the gusset and beam material had an elastic modulus of 29,000 ksi, a Poisson's ratio of 0.3, a yield stress of 50 ksi, and a post-yield modulus of 290 ksi (1% of elastic). A capping stress of 65 ksi was set, after which the material had negligible further hardening. The weld material in the FE model had an elastic modulus of 29,000 ksi, a yield stress of 70 ksi, and negligible further hardening. These material models, with nominal material strengths, were appropriate for comparison with design procedures that assumed nominal material strength.

The FE model was pushed to a point beyond where the beam shear mechanism was fully developed. Figure 4 shows the pushover curve, where the lateral force is the total applied load on the frame. Figure 4 shows six particular load points, and Table 1 summarizes the significance of each point. Figures 5 through 9 show stress and strain information corresponding to those particular points.

The evolution of the von Mises stress is shown in Figure 5. At a load of 616 kips [Figure 5(a)], there was a region of the beam web at midspan where the von Mises stress exceeded 50 ksi. This region propagated until it reached the extents of the gusset around 815 kips [Figure 5(d)]. At 873 kips [Figure 5(e)], the von Mises stress exceeded 50 ksi for a continuous region of the gusset plate between brace ends. The von Mises plot at 1024 [Figure 5(f)] shows regions with stresses over 55 ksi, reflecting strain hardening.

The evolution of the plastic strains is shown in Figures 6 and 7. At a load of 616 kips [Figure 6(a)], there were no plastic strains greater than 0.002. At 782 kips [Figure 6(c)], localized plastic strains in the beam coalesced to form a full-depth region of the beam web at midspan with plastic strain over 0.002. This plastic region expanded toward the gusset edges. At 873 kips [Figure 6(e)], most of the beam in the gusset region was plastic, as well as a region of the bottom gusset plate between the braces. Figure 7 shows closeup views of the gusset-to-beam weld at the same points. At 1024 kips [Figure 7(f)], the plastic regions of the weld extended 4 in. in from the ends of the weld (beam elements have a 1 in. dimension in the figure), and peak plastic strains exceeded 0.1.

Figure 8 shows the evolution of the shear stresses in the beam and gussets. In the beam, the shear stress exceeded

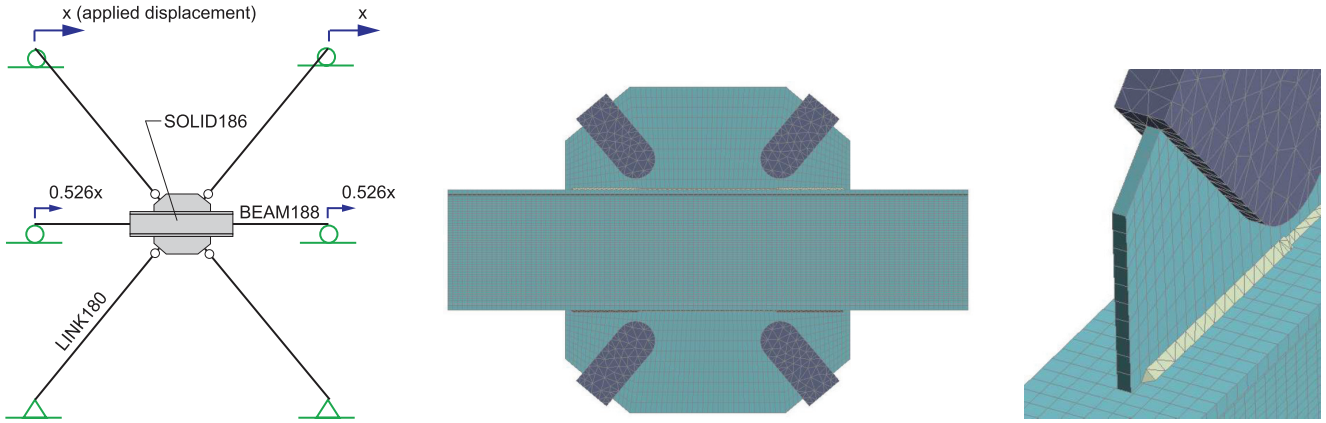

(a) Element types and boundary conditions

(b) Solid element mesh in the connection region

(c) Explicit modeling of the welds

Fig. 3. Finite element modeling techniques.

Table 1. Pushover Points for Discussion		
Point	**Load (kips)**	**Significance**
a	616	Von Mises stress exceeded 50 ksi in a localized region of the beam web.
b	744	Localized plastic strains exceeded 0.002 in the beam web and gusset-to-beam welds.
c	782	Localized plastic strains in the beam, over 0.002, coalesced to a full-depth region of the beam web.
d	815	Von Mises stress exceeded 50 ksi for a continuous region between braces in the bottom gusset. Change in tangent stiffness.
e	873	Shear stresses exceeded 30 ksi ($0.6F_y$) for a full-depth region of the beam web.
f	1024	Maximum load was applied.

25 ksi at midspan when the applied lateral load was 616 kips [Figure 8(a)], and the elevated region expanded as the loads increased. However, the shear stress in the beam web did not exceed 30 ksi through an entire section until the load was 873 kips [Figure 8(e)].

At all stages of loading, the shear stresses in the gusset were highest at midspan and decreased near the gusset ends. In fact, the shear stresses changed sign in the regions at the end of the gusset [Figure 8; signs changed at interface of light blue and medium blue], a finding that was documented in Richards et al. (2018). The gusset locations where the shear stress changed sign corresponded with the regions with high normal stress (Figure 9).

Figure 9 shows the evolution of *y*-direction normal stresses in the beam and gussets, which were generally low. For most regions, the normal stresses were between ±20 ksi throughout loading. For loading of 744 kips and above [Figure 9(b)–(f)], regions of concentrated normal stress (above 20 ksi) developed at the ends of the gusset plates. Normal stresses above 50 ksi developed at the highest levels of loading considered.

DISCUSSION

In the CSM example, the effective gusset length of 56 in. was selected to preclude beam yielding under a lateral force of 782 kips (the maximum force that could be delivered by the braces). If the CSM were accurate, the beam shear yielding limit state would be observed in the FE model at a load slightly greater than 782 kips.

The results in Figure 4 through 10 indicate that the beam shear yielding limit state was reached at a load a little greater than 782 kips. The pushover plot (Figure 4) shows softening around 782 kips that continued to develop

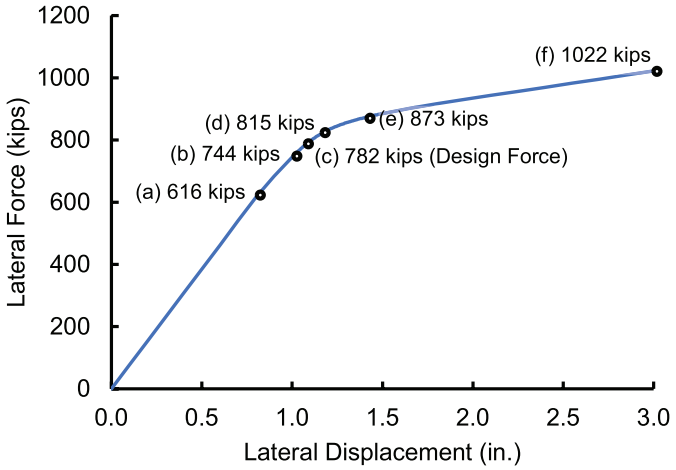

Fig. 4. Pushover curve for the finite element model.

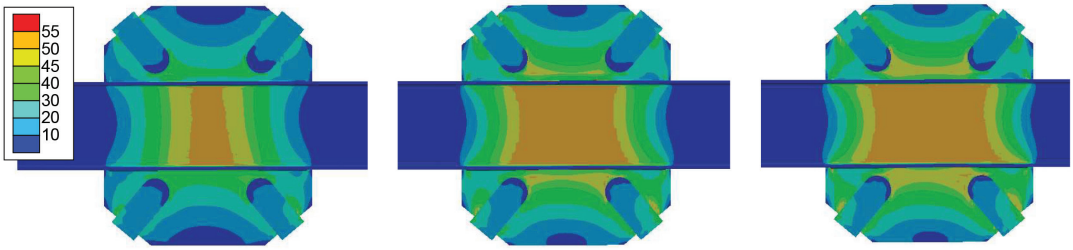

(a) 616 kips *(b) 744 kips* *(c) 782 kips*

(d) 815 kips *(e) 873 kips* *(f) 1024 kips*

Fig. 5. Equivalent (von Mises) stress (ksi) contours in the beam and gussets.

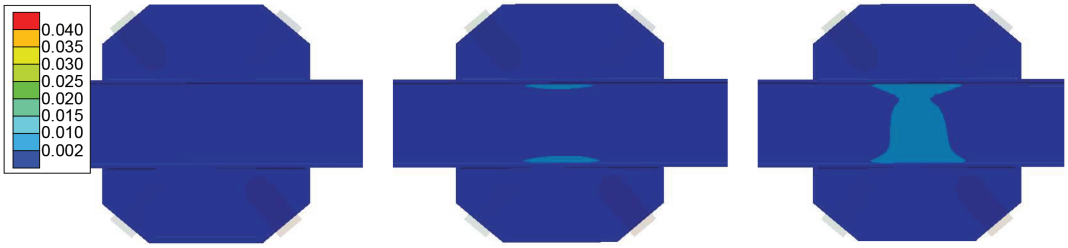

(a) 616 kips *(b) 744 kips* *(c) 782 kips*

(d) 815 kips *(e) 873 kips* *(f) 1024 kips*

Fig. 6. Plastic strain contours in the beam and gussets.

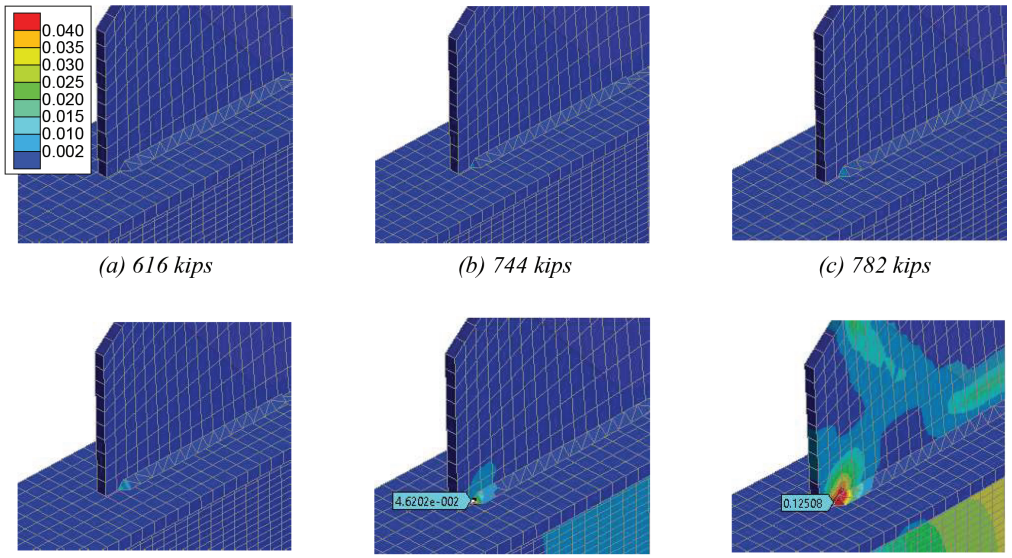

(a) 616 kips *(b) 744 kips* *(c) 782 kips*

(d) 815 kips *(e) 873 kips* *(f) 1024 kips*

Fig. 7. Plastic strains at the gusset-to-beam welds (beam flange elements have 1 in. edge length).

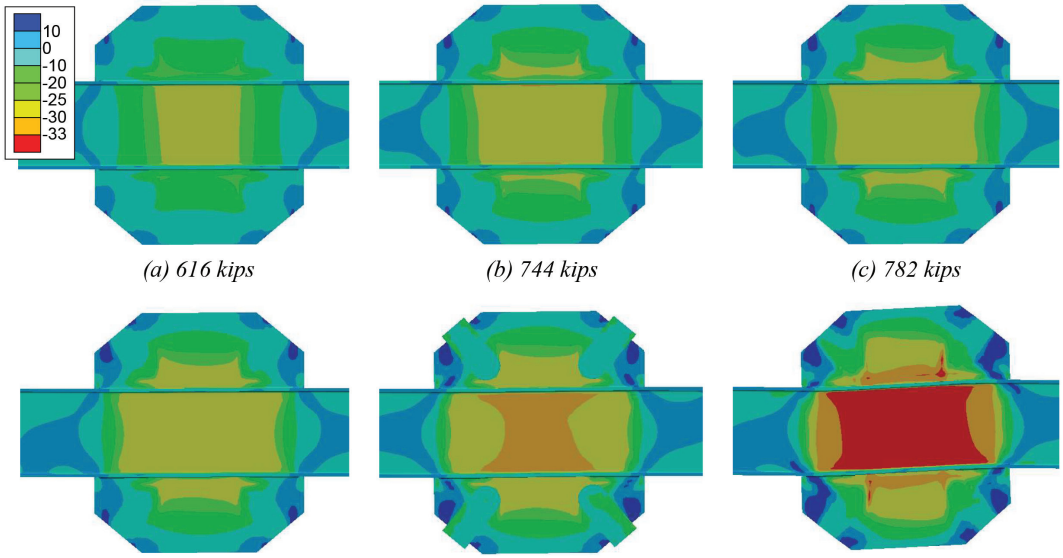

(a) 616 kips *(b) 744 kips* *(c) 782 kips*

(d) 815 kips *(e) 873 kips* *(f) 1024 kips*

Fig. 8. Shear stresses (ksi) in the beam and gussets.

to the stable post-yield stiffness by 873 kips. The plastic strain plot [Figure 6(c)] shows that at 782 kips, localized plastic strains above 0.002 had coalesced at the center of the beam. These strains propagated outward, with the beam web yielding being fully developed by 873 kips.

It is difficult to quantify precisely where the beam shear yielding limit state was reached, but Figure 10 offers additional insight. Figure 10 shows the tangent stiffness, k_t, normalized by the elastic stiffness $k_{elastic}$ for the different levels of lateral force. There appears to be an inflection point around 815 kips that suggests that the yielding is mature. As a sidenote for Figure 10, the stabilized post-yield stiffness (lateral forces greater than 900 kips) was about 10% of the elastic stiffness, even though the material hardening was only 1% of elastic because of the ratio of plastic beam rotation to story drift (to be discussed in the next section).

All these results support the conclusion that the CSM used by Sabelli and Saxey (2021) is reasonable for design.

The stress and strain contours in Figures 7 through 9 suggest some refinements for the CSM. In the CSM example,

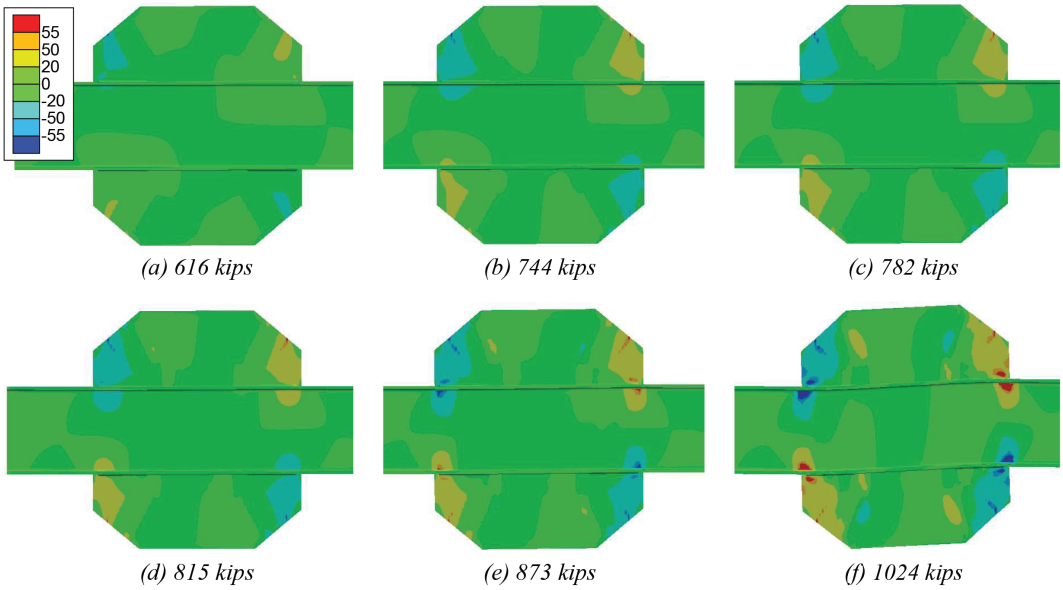

Fig. 9. Normal stresses (ksi) in the beam and gussets.

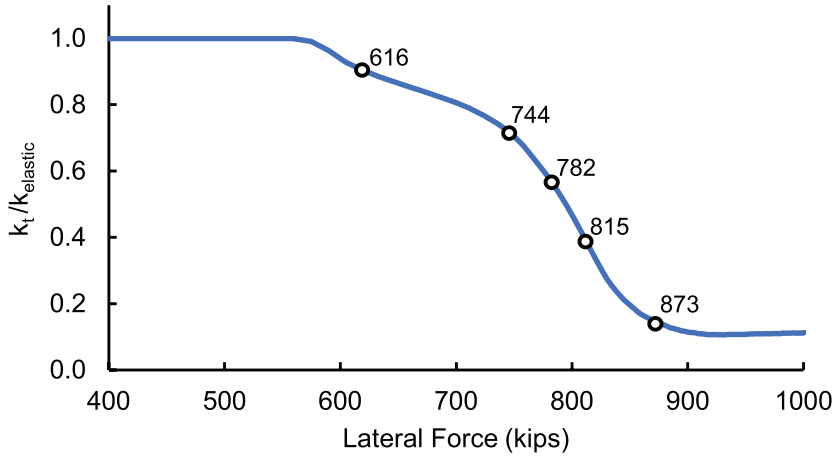

Fig. 10. Normalized tangent stiffness corresponding to various levels of lateral force.

a z_1 distance of 7.38 in. was used in design to designate the region of the gusset that is assumed to resist the moment at the connection through concentrated normal stresses. The FE model (Figures 7 and 9) indicated that the actual region of concentrated normal stress was somewhat smaller, more like 5.0 in. Another point of possible refinement is the assumption of the length that is effective for shear transfer. In the CSM example, the gusset-to-beam shear is assumed to be transferred evenly over the entire length of the gusset plate. The FE model demonstrated, as did Richards et al. (2018), that z regions did not transmit much shear. A refined CSM, with smaller z and shear transfer only in-between z regions, may better predict the demands on the gusset-to-beam welds.

BROADER DISCUSSION OF BEAM SHEAR YIELDING AND COMPARISON TO EBF

The CSM example frame would not be expected to experience significant beam yielding because the forces that could be delivered by the braces were lower than the forces required to reach the beam shear limit state. However, there may be other braced frames where local shear demands were not considered in the design and a beam yielding mechanism might occur. It is also possible that someone might contemplate a new seismic system that intentionally yields the beam. In those contexts, results about the extreme post-yield behavior of concentrically braced frames with beam yielding may be of interest.

The evolution of the shear stress in the beam web (Figure 8) is similar to that documented in experimental and finite element studies of shear-yielding links in eccentrically braced frames (EBF) (Hjelmstad and Popov, 1983; Richards et al., 2007). In discussing the post-yield behavior of a concentrically braced frame (CBF) with beam yielding, it is informative to compare and contrast with an EBF. An EBF FE model was developed to make comparisons with the CBF FE model as an academic exercise, see Figure 11.

The EBF model did not represent a code-compliant seismic design, just as the CBF model with a yielding beam did not represent a code-compliant seismic design. The purpose of the academic exercise was to compare and contrast beam yielding mechanisms. The EBF FE model had the same beam size (W24×94), beam length, and story heights as the CBF (Figure 5). The length of the shear link was 44 in. to match the observed intense yielding region in the CBF [Figure 5(f), red region]. The braces were modeled with elastic truss elements (infinitely strong, LINK180). As with the CBF model, the beam web and gusset plates were restrained against out-of-plane deformations, so stiffeners in the link beam or on the gussets were not necessary in the model. The nonlinear material properties for the beam were the same in the EBF model as they were in the CBF.

Figure 12 compares the inelastic pushover curves for both models. Results are shown up to an inelastic drift of 0.004. The lateral force that was required to yield the EBF was substantially lower than for the CBF with the same beam size because the eccentricity of the brace work points in the EBF was a more direct and effective way to impose shear on the beam web. Also, the CBF gussets help to carry some shear, as determined using the CSM. The lower post-yield stiffness in the EBF was a reflection of lower strains in the beam (less strain hardening).

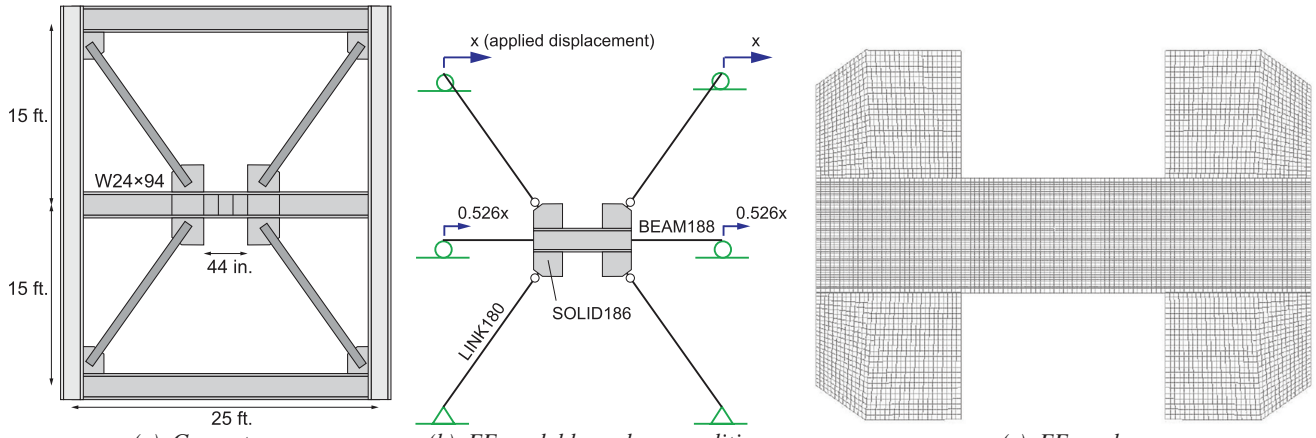

(a) Geometry (b) FE model boundary conditions (c) FE mesh

Fig. 11. EBF frame for comparison with the CBF.

Figure 13 compares the inelastic beam rotations versus the inelastic story drift for CBF and EBF. The EBF relationship between inelastic beam rotation and inelastic drift was within 13% of an estimate from a rigid plastic mechanism (Figure C-F3.4, AISC, 2016). The higher inelastic beam rotations for the CBF for a particular inelastic drift would make the CBF less attractive than EBF for an intentional beam yielding mechanism unless high post-yield stiffness were the primary aim.

Figure 14 compares the plastic strains and deformed geometries of both models at 0.004 rad inelastic story drift. The displacements have been scaled by a factor of 6 in both cases to illustrate the plastic mechanisms. The maximum web plastic strain in the CBF (0.035) is 75% more than the maximum plastic strain in the EBF (0.020) at the same inelastic drift. Also, the plastic strains are more uniformly distributed in the EBF.

The plastic mechanism in Figure 14 has the same form as the one postulated by Sabelli and Bolin (2022), where the plastic section of the beam is less than the full length of the gusset. The plastic strains in the gusset in Figure 14(a), including the concentrations of strain at the ends, illustrate the gusset/weld deformations required for compatibility with the yielding beam.

This academic exercise demonstrates that it is theoretically possible to design a CBF with a beam yielding mechanism, even though current seismic design provisions do not allow it. There are advantages and disadvantages of CBF

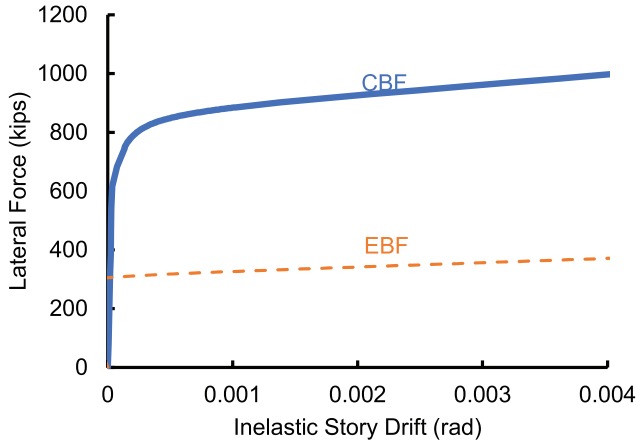

Fig. 12. Inelastic story drift vs. lateral force for CBF and EBF.

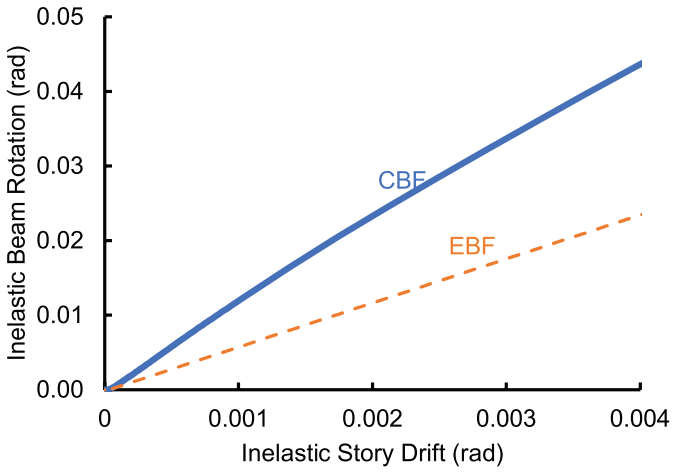

Fig. 13. Inelastic beam rotation vs. inelastic story drift for CBF and EBF FE models.

with beam yielding as compared to an EBF. The CBF advantages are greater elastic stiffness, strength, and post-yield stiffness. The CBF disadvantages are higher beam rotation and higher beam strains to achieve a particular inelastic drift (although less inelastic drift might be required for a CBF since the elastic stiffness is greater).

If existing chevron frames have been unintentionally designed such that yielding would occur in the beam web, these analyses demonstrate the expected plastic mechanism.

CONCLUSIONS

A finite element (FE) model was developed to investigate the design procedure presented by Sabelli and Saxey (2021). The braces in the model had unlimited strength to force a beam-yielding mechanism to occur. A pushover analysis was performed to check if the Concentrated Stress Method (CSM) used by Sabelli and Saxey (2021) in their CSM example was accurate in predicting the beam shear yielding limit state. Here are the conclusions from the exercise:

- The CSM used by Sabelli and Saxey (2021) was reasonable for design. The FE model confirmed that the CSM example frame would not have experienced a beam yielding limit state under the design forces (maximum forces that could be delivered by the braces).
- While there was not a clear method for defining when the beam yielding limit state was reached in the FE model, an inflection point for the tangent stiffness suggested about 815 kips, which was 4% higher than the design force used in the CSM example.
- The method for estimating the z regions in the CSM example might be refined. A higher value for z was used in the CSM example than observed in the FE model.
- The method for assigning regions of the gusset to transmit shear in the CSM example might be refined. In the CSM example, shear was assumed to be transmitted along the entire length of the gusset, but the FE models indicate the z regions are not effective for shear transfer.

An additional FE model of an EBF was used for an academic exercise, comparing the post-yield plastic mechanism of a CBF (with beam yielding) with an EBF with the same beam. This discussion was outside the scope of Sabelli and Saxey (2021) but pertinent to the broader topic of local member shear demands. Conclusions were as follows:

- The CBF FE model developed the plastic mechanism discussed by Sabelli and Bolin (2022) and confirmed their assumption that the yielding region of the beam was shorter than the total gusset length.
- The shear yielding mechanism in the CBF beam (when braces had unlimited strength), was similar to an EBF shear link; however, the lateral forces to trigger the mechanism were much higher for the CBF. At the same inelastic story drift, the inelastic beam rotation and plastic strains were higher in the CBF with beam yielding than in the EBF with the same beam size.

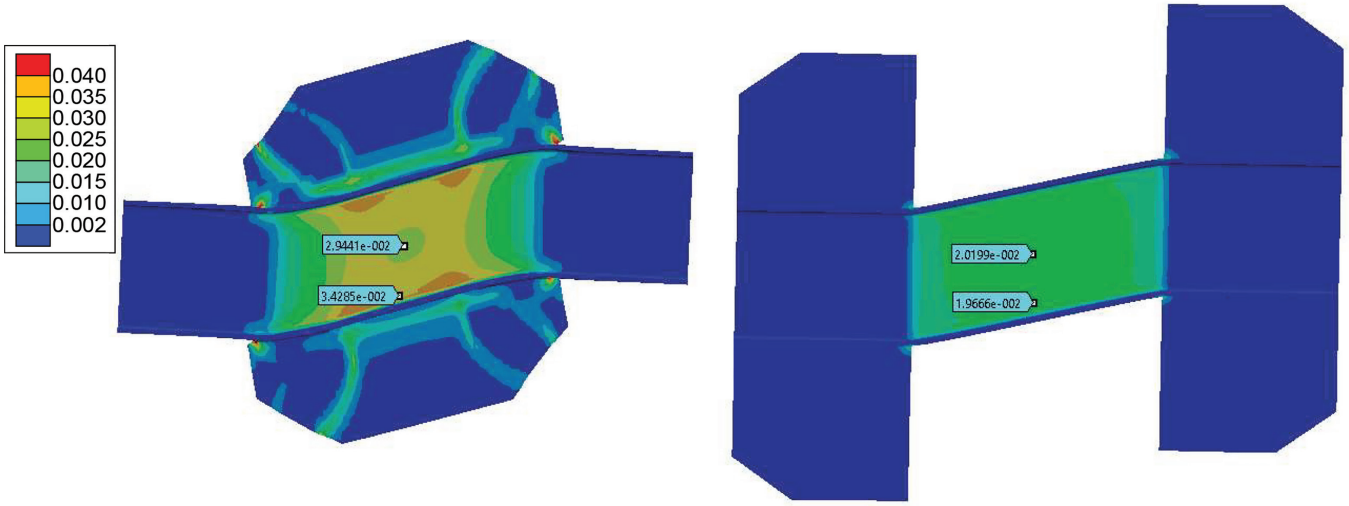

(a) Chevron *(b) EBF*

Fig. 14. Plastic strains in the chevron and EBF models at 0.004 rad inelastic story drift.

REFERENCES

AISC (2016), *Seismic Provisions for Structural Steel Buildings*, ANSI/AISC 341-16, American Institute of Steel Construction Chicago, Ill.

ANSYS (2022), Ansys Mechanical, Release 22.1, Help System, ANSYS, Inc.

Fortney, P.J. and Thornton, W.A. (2015), "The Chevron Effect—Not an Isolated Problem," *Engineering Journal*, Vol. 52, No. 2, pp. 125–164.

Fortney, P.J. and Thornton, W.A. (2017), "The Chevron Effect and the Analysis of Chevron Beams—A Paradigm Shift," *Engineering Journal*, Vol. 54, No. 4, pp. 263–296.

Hadad, A.A. and Fortney, P.J. (2020), "Investigation on the Performance of a Mathematical Model to Analyze Concentrically Braced Frame Beams with V-Type Bracing Configurations," *Engineering Journal*, Vol. 57, No. 2, pp. 91–108.

Hadad, A.A. and Thornton, W.A. (2022), "Closure: Investigation on the Performance of a Mathematical Model to Analyze Concentrically Braced Frame Beams with V-Type Bracing Configurations," *Engineering Journal*, Vol. 59, No. 1, pp. 1–4.

Hjelmstad, K.D. and Popov, E.P. (1983), "Cyclic Behavior and Design of Link Beams," *Journal of Structural Engineering*, Vol. 109, No. 10, pp. 2,387–2,403.

Richards, P.W., Miller, B., and Linford, J. (2018), "Finite Element Evaluation of the Chevron Effect in Braced Frames," SSRP-2018/02, Brigham Young University, Provo, Utah.

Richards, P., Okazaki, T., Engelhardt, M., and Uang, C.-M. (2007), "Impact of Recent Research Findings on Eccentrically Braced Frame Design," *Engineering Journal*, Vol. 44, No. 1, pp. 41–53.

Roeder, C.W., Lehman, D.E., Tan, Q., Berman, J.W., and Sen, A.D. (2021), "Discussion: Investigation on the Performance of a Mathematical Model to Analyze Concetrically Braced Frame Beams with V-Type Bracing Configurations," *Engineering Journal*, Vol. 58, No. 1.

Sabelli, R. and Bolin, E. (2022), "The Chevron Effect: Reserve Strength of Existing Chevron Frames," *Engineering Journal*, Vol. 59, No. 3, pp. 209–224.

Sabelli, R. and Saxey, B. (2021), "Design for Local Member Shear at Brace and Diagonal-Member Connections: Full-Height and Chevron Gussets," *Engineering Journal*, Vol. 58, No. 1, pp. 45–78.

Sabelli, R., Saxey, B., Li, C.-H., and Thornton, W. A. (2021), "Design for Local Web Shear at Brace Connections: An Adaptation of the Uniform Force Method," *Engineering Journal*, Vol. 58, No. 4, pp. 223–266.